FERMILAB-Proposal-0728

Fermilab

November 1, 1982

Ref. P-712

Norman Gelfand, Secretary
The Physics Advisory Committee
Fermilab

Dear Norman,

We intend to resubmit P-712 by February 1, 1983. Our proposal is to add muon detection and hadron calorimetry to the LAPDOG detector. Our interest in leptons led us rather naturally to approach the LAPDOG group with an eye to integration of the two detectors. During joint discussions between the two groups it very quickly became apparent that there was a lot to be gained for both groups; clearly the combined detector is much more powerful than the simple sum of the two. The LAPDOG group has responded positively to this idea and encouraged us to pursue it.

Our proposed muon-detector does not seal up LAPDOG in a tomb. It in no way compromises them. The obvious advantages to them are that a natural way to provide radiation shielding from beam gas interactions is provided, and that the crude hadron calorimetry incorporated in our muon detector will improve their $e/\pi$ separation. This latter point will be discussed in more detail below. It is clear to both the P-712 and P-714 groups that if both detectors are approved then we will integrate them electronically and mechanically into a single powerful detector built and exploited for physics by a single group.

We feel the same sorts of time pressures discussed by P-714 in their letter - competition from other accelerators, long lead time in designing and ordering the components of this large system, and design and construction of the DØ experimental area which cannot really start seriously until an experiment(s) is/are approved. Therefore, we urge an early decision.

Lepton production will be measured at the FNAL collider as a function of $\sqrt{s}$ and $P_\perp$. Topological cuts will be used to separate and study prompt and electroweak muons at high $P_\perp$. These topological cuts will arise from crude charged particle calorimetry supplied by our apparatus and fine grained neutral particle calorimetry supplied by the "core detector" - LAPDOG. These combined detectors will study multileptons with charge information. This technique will be a powerful probe of heavy flavor production processes, as well as electroweak production processes. An elevation view schematic of the detector is shown in Fig. 1.

88pages

## The Central Region $45^{\circ} \leq \theta \leq 135^{\circ}$

We consider $90^{\circ}$ muons to be important for possible new phenomena. Basically, we have opened up and thinned the P-712 geometry to accommodate a compact "core detector". The geometry is still "closed" with respect to CDF. However, we win back more than we lose by the use of topological cuts provided by using the tracking and neutral particle energy information of the "core detector" and the energy deposition in the depth segmented muon detector. Rates and backgrounds for W decays are shown in Fig. 3. An integrated luminosity of $\int Ldt = 10^{36} cm^{-2}$ is assumed.

An objection from the PAC has been that P-712 does not see anything but the muons. This objection is indeed valid and we have opened up the P-712 geometry to accommodate the LAPDOG detector as a core detector. This detector will provide wide angle tracks, information on angles and neutral momentum and F/B information on angle, momentum and charge. This information provides very powerful rejection of background jet events which improve the experiment over P712. However, we still maintain a compact closed geometry with sufficient thickness so as not to be swamped with false triggers. We feel that this compact geometry is an optimal compromise between an open setup and a totally closed (and hence blind) layout.

In the central region, our decay path is less than that of CDF and our number of absorption lengths is larger. In the light of the UA1 proposal to add additional magnetized iron absorbers in order to achieve an acceptable trigger rate, we consider these advantages to be crucial. UA1 needs a factor 10 in trigger rate reduction and proposes (CERN/SPSC/82-51) to add 3.5 $\lambda$ to their existing 5.8 $\lambda$. By comparison, CDF has ~5 $\lambda$ and P712 (with P714) has ~9-10 $\lambda$. Thus, the initial SPS collider experience has confirmed our assertion that detector thickness is very important.

## Detector "Building Blocks"

The previous toroidal geometry of P712 completely encapsulated the inner core, and implied a field direction which was poor for triggering purposes. Our new geometry consists of stacks of "building blocks", as shown in Fig. 2, which are completely self contained. This geometry allows us to easily assemble the detector, access the core detector, orient the field direction more advantageously (as in the initial version of P-712), and more easily segment the steel in depth. Stray field problems will be negligible since the magnetic flux is entirely contained in the "building block". Clearly, the adoption of this configuration has strengthened P712 significantly.

## Depth Segmentation of the μ Detectors

We have decided to depth segment the detector absorber for several reasons. The "building block" approach frees us to do this. Sampling the trajectory will allow us to reduce the triggers due to interactions and subsequent punch-through to a low level. In addition, crude resolution, coarse grained measurements of hadron energy will provide two additional constraints. First, topological rejection of jets will be enhanced over the rejection available from neutral particle energy alone. Second, the LAPDOG e/π hadronic rejection will be improved by sampling the shower development after the track exits from the rather thin ($\lambda \sim 2$) LAPDOG detector. Three samples at depths of 1, 2, and 3 λ are sufficient for these purposes. The segmentation in depth and the solid angle granularity in $(\theta,\phi)$ are crude as regards calorimetry. Rather, the detector will reduce μ triggers, improve e cleanliness and provide modest additional topological rejection factors. We do not intend P712 to do fine calorimetry a la CDF, merely to do one job very well - lepton physics.

## Forward/Backward Region

The F/B region ($5^{\circ} \lesssim \theta \lesssim 30^{\circ}$ , $150^{\circ} < \theta < 175^{\circ}$) has a lower rate and higher background for W physics than the central region. Naturally, seeing both leptons in both arms gives one an effective increase in luminosity. The F/B electroweak asymmetry is a crucial handle on $W^{\pm}$ production. We feel that both an F arm and a B arm are needed to fully exploit the expected asymmetry. Azimuthal acceptance is a full 2 π.

We consider that detecting 2 leptons in 2 arms is crucial for avoiding systematic errors in measuring asymmetries. The rates and backgrounds are shown in Fig. 3, while the asymmetry is shown in Fig. 4. Clearly, the combination of short decay length, thick absorber, dual independent momentum measurements (as in E605), and powerful topological cuts makes this physics accessible to P712. Combined with LAPDOG, both electron and muon asymmetrics are measured in the same apparatus. This fact should reduce systematic errors.

## Decay Background

The background from $\pi \to \mu$ decays is increased by a factor $\sim 5$ over that of our previous proposal. However, this loss is more than recouped by topological cuts. For $P_{\perp} \gtrsim 20$ GeV/c one gets a factor $\gtrsim 10$ rejection by requiring little accompanying neutral energy (toward cut) and another factor $\gtrsim 10$ rejection requiring missing $P_{\perp}$ (away cut). We feel these factors are rather conservative in that one can see the $W^{\pm} \to \mu^{\pm} \nu$ Jacobian peak without them (see Fig. 3) and in that we have not used the segmented iron information in evaluating them. The decay rejection factor is $\sim 2000$ for both central and F/B regions at $P_{\perp} \sim 30$ GeV/c.

## Punchthrough Background

As mentioned above, CDF has ~5 λ and P712 has ~9-10 λ. This implies a factor ~60 less non-interacting punchthrough in P712. Interacting punchthrough is removable at the analysis level by tight constraints on a match between incoming and outgoing positions and angles - the "Coulomb telescope". However, as experienced by UA1, one can be swamped at the trigger level if one's detector is too thin. Note also, that the added UA1 iron is magnetized. The second independent momentum measurement (which we have in the more difficult F/B region) is of use in further tightening the constraints on matching incoming and outgoing phase space.

We expect that interacting punchthrough can be reduced offline to negligible levels with respect to non-interacting punchthrough. The absorber lengths were chosen to be L = 130 (150) cm so as to have $\lesssim 1$ particle emerging per entering particle at $P_\perp = 30$ GeV/c for the central (F/B) detectors. The rejection factor is ~7500 (49,000) for the central (F/B) detector.

## Momentum Measurement

We have chosen lever arms of $\ell = 40$ (60) cm so as to have errors dominated by multiple scattering for $P_\perp \lesssim 100$ GeV/c. Our resolution is $(\delta P/P) = \pm 0.15$ ($\pm 0.19$) for the F/B (central) regions assuming only a 14 KG field. This resolution is adequate in most models of the Jacobian "peak" (F. Paige, BNL 30805). In the F/B detectors this resolution will be comparable to and independent of the P714 momentum resolution at $P_\perp \sim 30$ GeV/c. Measuring momentum twice and measuring energy deposition in both the lead glass and the depth segmented iron will serve to clean up residual backgrounds.

## Multileptons and Heavy Quark Physics

LAPDOG is aided by the P712 hadronic energy measurements for $e/\pi$ rejection and for topological rejection. In addition, the F/B detectors double the effective luminosity for lepton asymmetry measurements. The F/B detectors also shield the P714 lead glass from beam · gas energy deposition. In addition multilepton production can be studied with charge information on the muons for $5^\circ < \theta < 175^\circ$ and charge of

the electrons for $5^\circ \lesssim \theta \lesssim 25^\circ$ and $175^\circ < \theta < 155^\circ$. This information is interesting in its own right as a probe of heavy quark production. It will also provide, (in a statistical and model independent way) a subtraction of heavy quark yields from the electroweak signal of interest, either in the single lepton $W^\pm$ signal (P712 - $\mu^\pm$, P714 - $e^\pm$) or in the dilepton $Z^0$ signal should backgrounds prove more difficult than expected. "Prompt" leptons from heavy quark decays dominate $\pi \to \mu$ decay backgrounds for $P_\perp \gtrsim 20$ GeV/c. Thus, one can study heavy flavor production by using anti-topological cuts. Like - sign dileptons signal heavy flavors, e.g., $\mu^\pm e^\pm$, $\mu^\pm \mu^\pm$, $e^\pm e^\pm$.

## The Detector

A polar section of half the detector is shown in Fig. 1. In the central region each of the 4 sides has a wall of magnetized and instrumented steel backing up the lead glass P714 detector. Each wall has at least 4 feet of absorber comprised of 8 inch thick plates. The basic building blocks (shown in Fig. 2) facilitate access to the "core detector". Showers are sampled with either scintillator or gas calorimetry after each of the first three layers. These sampling sections can also be used at the trigger level (along with core detector tower signals) to impose the condition that the track did not interact for the first 5 $\lambda$. Tracking will be done as in the previous P712 version with proportional tubes operated in the drift mode.

For the F/B regions the approach is much the same except the field is toroidal. The air toroids and tracking chambers of P714 measure angles and momentum. Shower development is measured in P714 lead glass for 2$\lambda$ and then in P712 steel for 3$\lambda$. The steel is thicker than the central region to accommodate the higher momentum secondaries which punchthrough deeper. A beam view of a toroid is shown in Fig. 5. The center hole is cut to accommodate low $\beta$ quadrupoles and to protect the main ring pipe with a current sheet. Additional magnetic shielding can be provided if necessary. Momentum information is provided by drift tube tracking. Thus the momentum is measured twice, independently, in recognition that the F/B region is more difficult than the central region for leptons.

The total weight of steel is estimated at 1100 tons in the central detector and 500 in the F/B detectors. A rough cost estimate is \$2 M for the experiment, of which the major portion is for the high quality steel necessary for the "building block" type of construction. The volume of the apparatus is within the 750 $m^3$ guideline for the DØ area. Clearly, this is a modest increment to the TeV I and CDF total costs.

The regions $25^o \lesssim \theta \lesssim 45^o$ and $135^o \lesssim \theta \lesssim 155^o$ are obviously holes in the detectors. Equally obvious is the fact that these regions must be considered in the context of a detailed engineering integration of P714 and P712 taking into account installation and maintenance requirements.

## Conclusion

Neither LAPDOG nor P712 would be compromised by the proposed merger. The combined apparatus would be a powerful tool to explore leptonic physics at the Fermilab collider and be complimentary to the CDF program and capabilities.

We feel that DØ is indeed very serious real estate; it represents probably half of all U.S. hadronic collider physics for the near future. As such, it would be ludicrous to be in a situation that DØ not be ready with a debugged experiment for the first collision. This seems to us particularly clear considering the minor cost of DØ in relation to BØ and the Saver/Collider.

Sincerely yours,

Dan Green

Dan Green, Fermilab
for the P-712 group

P-712 group:

John Ficenec, Virginia Polytechnic Institute
Harvey Goldman, Florida State University
Dan Green, Fermilab
Herman Haggerty, Fermilab
Ernest Malamud, Fermilab
Burt Pifer, University of Arizona
Pat Rapp, University of Maryland

attached:

Fig. 1: Elevation view of the detector

Fig. 2: Magnet building block, central detector

Fig. 3: $W^{\pm} \rightarrow \mu^{\pm}$ rates
- a) into F or B detector
- b) into central detector. The backgrounds are due to $\pi$ decays, $\pi$ punchthrough, and prompt leptons from heavy flavor decay

Fig. 4: F/B asymmetry
- a) rate into F or B detector as in Fig. 3a but with background added to signal
- b) asymmetry expected as a function of $P_{\perp}$ with and without background

Fig. 5: Cross section of the F(B) toroid illustrating inner current sheet shielding the beam pipes from stray magnetic fields.

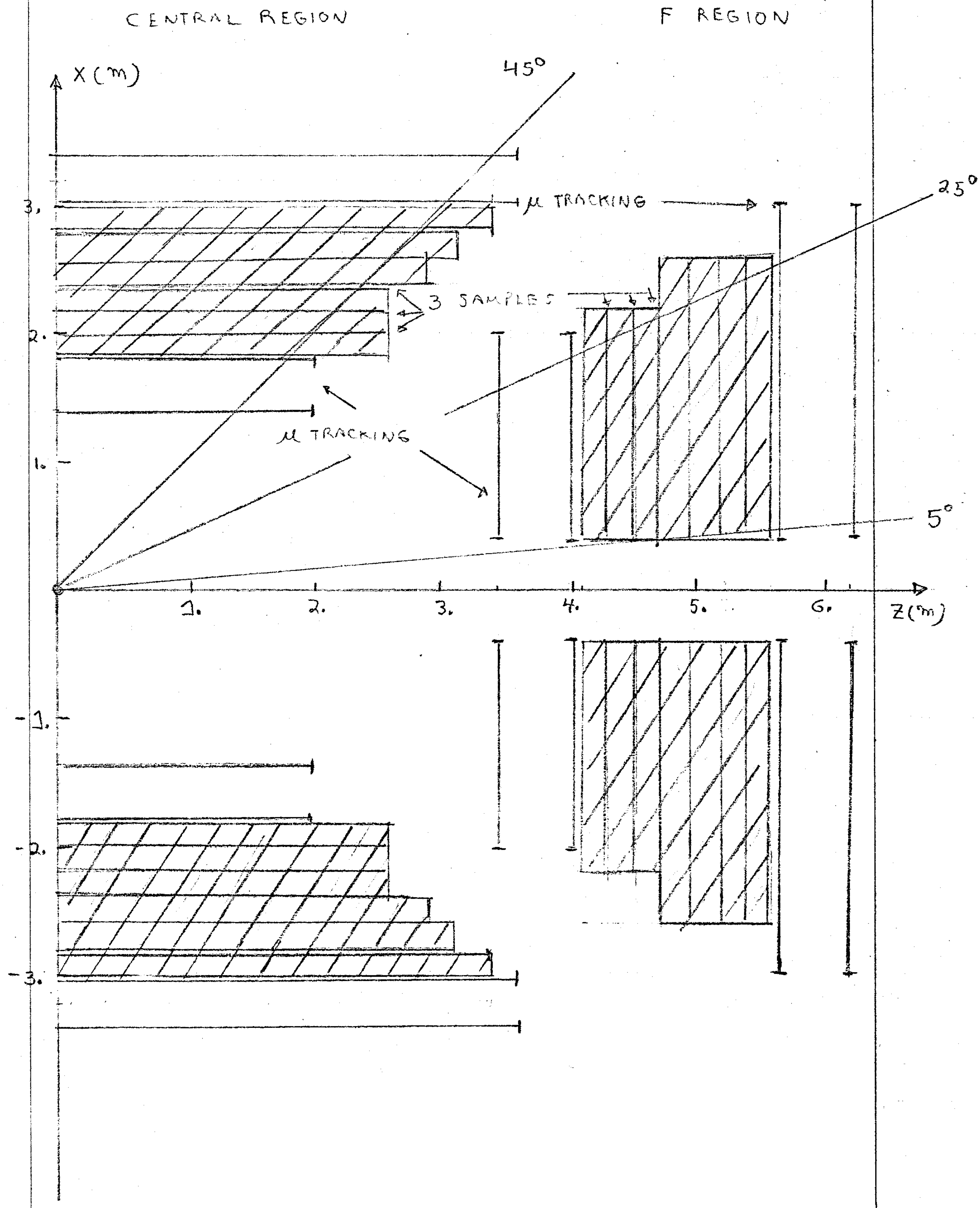
CENTRAL REGION
F REGION
X (m)
45°
25°
5°
μ TRACKING
3 SAMPLES
μ TRACKING
3.
2.
1.
-1.
-2.
-3.
1.
2.
3.
4.
5.
6.
Z (m)

FIG 2

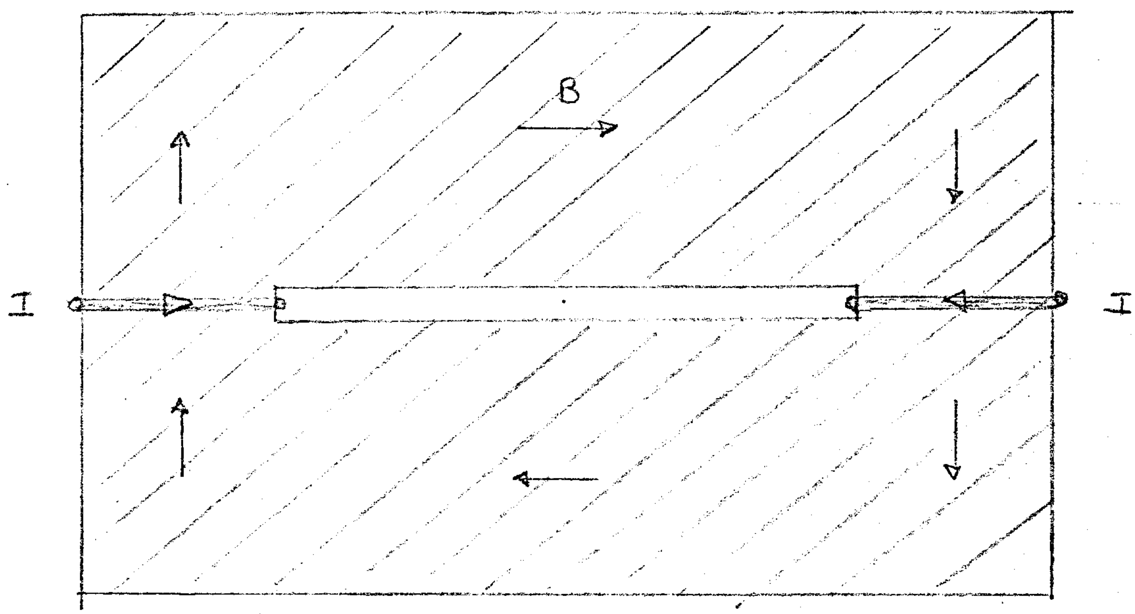

FIG 3

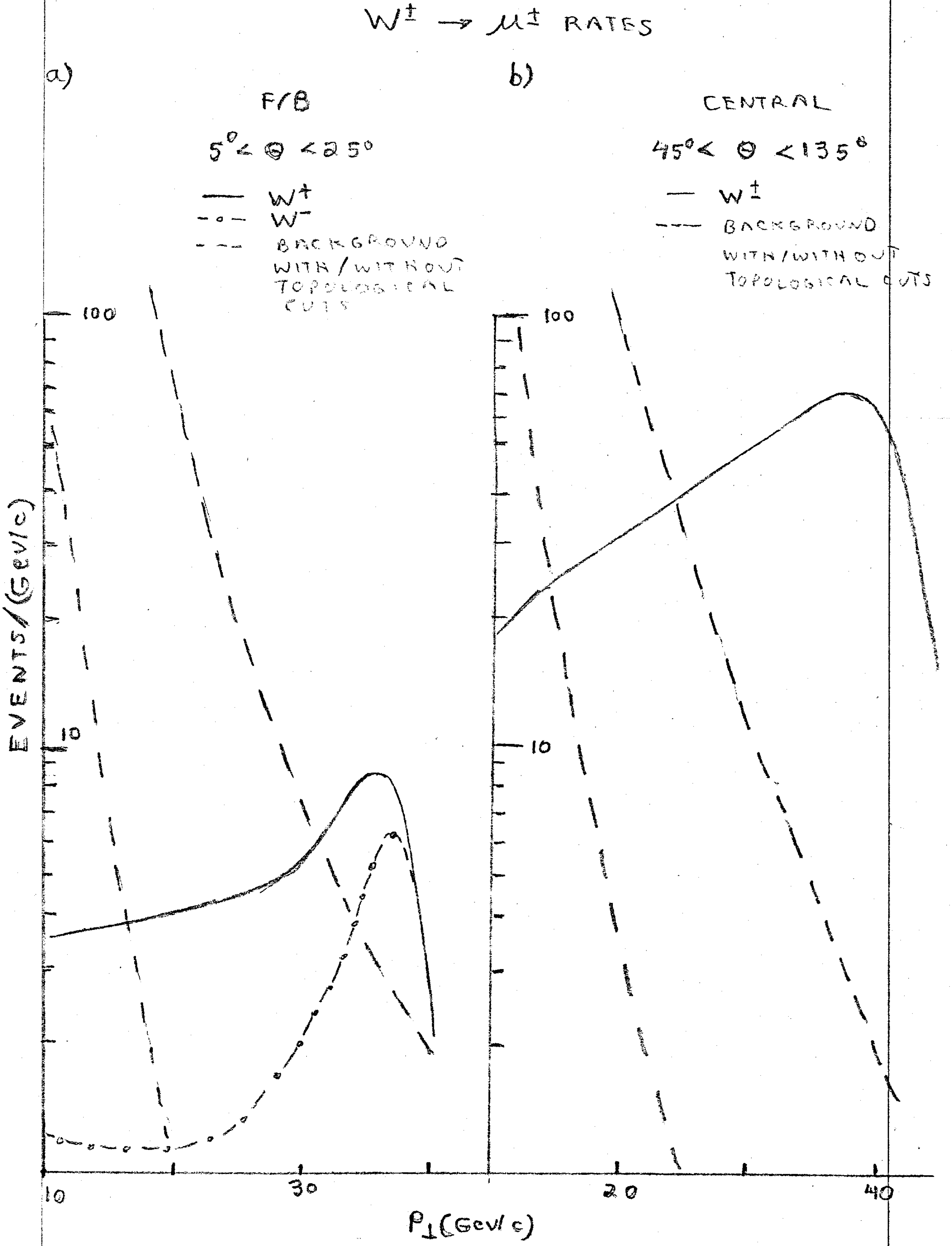
W± → μ± RATES
a)
F/B
5° < Θ < 25°
W+
W−
BACKGROUND
WITH/WITHOUT
TOPOLOGICAL
CUTS
b)
CENTRAL
45° < Θ < 135°
W±
BACKGROUND
WITH/WITHOUT
TOPOLOGICAL CUTS
100
10
EVENTS/(GeV/c)
10
30
20
40
P⊥(GeV/c)

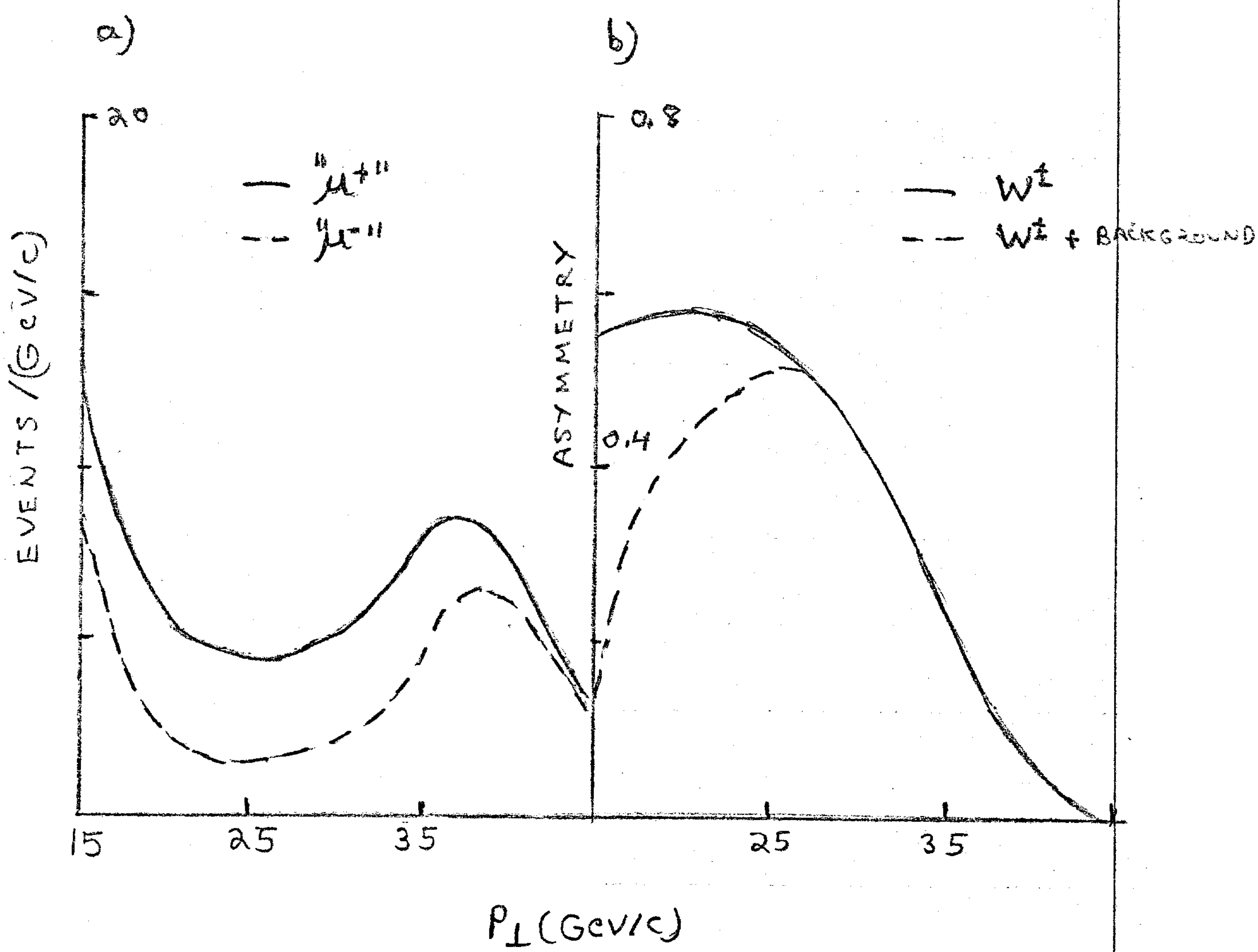
a)
b)
20
0.8
0.4
"μ+"
"μ-"
W±
W± + BACKGROUND
EVENTS /(GeV/c)
ASYMMETRY
15
25
35
25
35
P⊥(GeV/c)

FIG 5

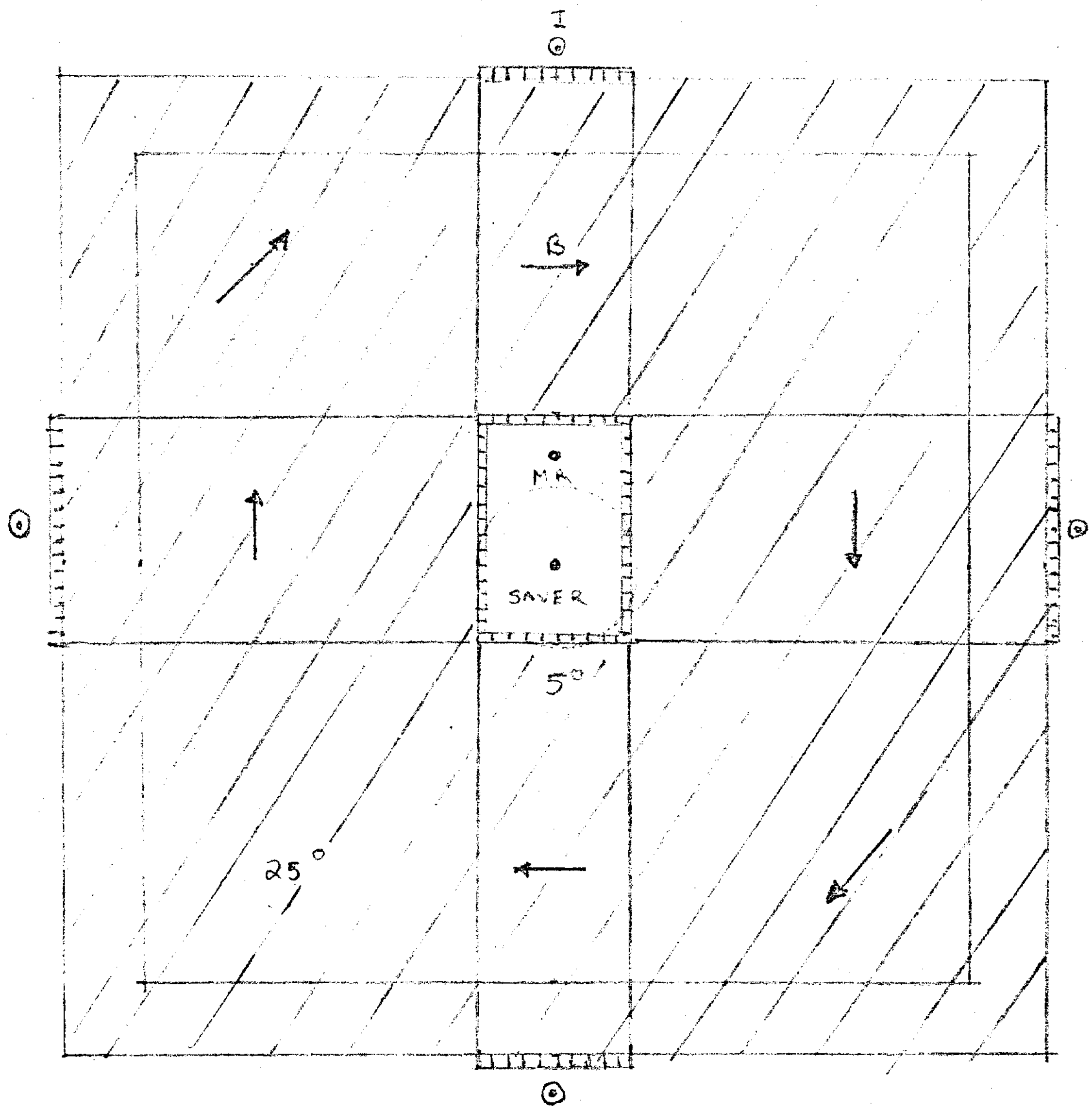

Fermilab Proposal No. 728

Scientific Spokesperson: Dan Green
Fermilab
Phone: (312) 840-3104
FTS 370-3104

# STUDY OF MUONS FROM $\bar{P}P$ COLLISIONS UP TO $\sqrt{s}=2$ TeV

A. E. Pifer
University of Arizona

D. Green, H. Haggerty, E. Malamud
Fermilab

H. Goldman
Florida State University

P. Rapp
University of Maryland

J. Ficenec
Virginia Tech

February 1, 1983

CONTENTS



Appendices

Abstract

We propose a simple apparatus for detection of single and multiple muons emerging from the D0 colliding region. The copious background muon sources inherent in general purpose detectors suggest a special purpose closed-geometry detection scheme. The detector, constructed from magnetized steel blocks and instrumented with drift tubes and scintillator, is proposed to back up the LAPDOG (P-714) e,$\gamma$ detector both in the central region and in the forward/backward regions. The combined apparatus will be a powerful tool to explore lepton-photon physics at the Fermilab collider and will complement the CDF program and capabilities. We will measure the production of muons from the FNAL collider as a function of $\sqrt{s}$ and $p_t$. Our trigger background from punch-through and pi decay is below that for CDF, allowing any muon signal to be more cleanly seen. This will be especially important if the pion background is larger than expected or if the production of heavy masses is more momentum smeared than expected.

## I. Introduction

The CDF group has done an elegant and thorough job of outlining the overall motivation for studying collisions at $\sqrt{s}=2$ TeV[1]. Our feeling is that a general purpose detector must make compromises. In particular, the physics inherent in prompt muon detection is of such interest as to make the optimal design of a special purpose closed- geometry muon detector attractive. We propose to build an optimized muon detector in the D0 collision hall. Our interest in leptons led us rather naturally to approach the LAPDOG group (P-714) with an eye to integration of the two detectors. During joint discussions between the two groups it very quickly became apparent that there was a lot to be gained for both groups; the combined detector is much more powerful than the simple sum of the two. The LAPDOG group has responded positively to this idea and encouraged us to pursue it. A letter from them is attached as Appendix A.

Our proposed muon detector does not compromise LAPDOG in any way. The advantages to them are that a natural way to provide radiation shielding from beam gas interactions is provided, and that the crude hadron calorimetry incorporated in our muon detector will improve their $e/\pi$ separation and the view of event topology, to be discussed in more detail below. It is clear to both the groups that if both detectors are approved then we will integrate them electronically and mechanically into a single powerful detector built and exploited for physics by a single group.

We consider $90^{o}$ muons to be important for possible new phenomena. Basically, we have opened up the geometry to accommodate a compact "core detector" such as LAPDOG. The geometry is still "closed" with respect to CDF. However, we win back more than we lose by the use of topological cuts provided by using the tracking and neutral particle energy information of the "core detector" and the energy deposition in the depth segmented muon detector. The LAPDOG detector will provide tracking of charged particles and energy of electrons and photons. This information is sufficient for rejection of background jet events. However, we maintain a compact closed geometry with sufficient thickness so as not to be swamped with false triggers, yet thin enough to yield data overlapping the known $p_t$ regime. We feel that this geometry is is an optimal compromise between an open setup and a totally closed (and hence blind) experiment.

In the central region, our decay path is less than that of CDF and our number of absorption lengths is larger. In the light of the UA1[2] plan to add additional magnetized iron absorbers in order to reduce the trigger rate, we consider these advantages to be crucial.

Our geometry consists of stacks of magnetized iron "building blocks" which are completely self contained. This geometry allows us to easily assemble the detector, access the core detector, orient the field direction more advantageously and more easily segment the steel in depth. Stray field problems will be negligible since the magnetic flux is entirely contained in the "building block".

We have decided to depth segment the detector absorber for several reasons. Sampling the trajectory will allow us to study the triggers due to interactions and subsequent punch-through to a low level. In addition, crude resolution, coarse grained measurements of hadron energy will provide two additional constraints. First, topological rejection of jets will be enhanced over the rejection available from neutral particle energy alone. Second, the LAPDOG $e/\pi$ hadronic rejection will be improved by sampling the shower development after the track exits from the rather thin ($\lambda=2$) LAPDOG detector. Three samples in our detector at depths of 1, 2, and $3\lambda$ are sufficient for these purposes. The segmentation in depth and the solid angle granularity in $(\theta,\phi)$ are crude as regards calorimetry. Rather, the detector will reduce $\mu$ triggers, improve e cleanliness and provide modest additional topological rejection factors.

The F/B region ($5^o<\theta<30^o$ ,$150^o<\theta<175^o$ ) has a lower rate and higher background for W physics than the central region. Naturally, seeing <u>both</u> leptons in <u>both</u> arms gives one an effective increase in luminosity. The F/B electroweak asymmetry is a crucial handle on $W^{\pm}$ production. We feel that both an F arm and a B arm are needed to fully exploit the expected asymmetry. Azimuthal acceptance is $2\pi$. The combination of short decay length, thick absorber, dual independent momentum measurements (as in E-605), and powerful topological cuts makes this physics accessible to P-714/728. Combined with LAPDOG, both electon and muon asymmetries are measured in the same apparatus. This fact should reduce systematic errors. Multilepton production can be studied <u>with</u> charge information on the muons for $5^o<\theta<175^o$ and with charge information on the electrons for $5^o<\theta<25^o$ and $175^o<\theta<155^o$. This information is interesting in its own right as a probe of heavy quark production. It will also provide, (in a statistical and model independent way) a subtraction of heavy quark yields from the electroweak signal of interest, either in the single lepton $W^{\pm}$ signal or in the dilepton $Z^o$ signal should backgrounds prove more difficult than expected. "Prompt" leptons from heavy quark decays dominate $\pi\to\mu$ decay backgrounds for $p_t>20$ GeV/c. Thus, one can study heavy flavor production by using topological cuts. Like-sign dileptons signal heavy flavor, and like sign trimuons signal heavy flavors.

In the central region each of the 4 sides has a wall of magnetized and instrumented steel at least 4 feet thick backing up the lead glass P-714 detector. The basic building blocks facilitate access to the "core detector". Showers are sampled with either scintillator or gas calorimentry after each of the first three layers (along with core detector tower signals) to impose the condition that the track did not interact for the first 5λ. Tracking will be done with "proportional tubes" operated in the drift mode.

For the F/B regions the approach is much the same except the field is toroidal. The air toroids and tracking chambers of P-714 measure angles and momentum. Shower development is measured in P-714 lead glass for 2λ and then in P-728 steel for 3λ. The steel is thicker than the central region to accomodate the higher momentum secondaries which punch through deeper. The center hole accomodates low β quadrupoles and protects the main ring pipe with a current sheet. Additional magnetic shielding can be provided if necessary. Momentum is measured twice, independently, in recognition that the F/B region is more difficult than the central region for leptons.

# I. Physics Motivation

## A. Electroweak Boson Production

The production cross section for $W^{\pm}$ and decay branching ratios are taken to be[3]

$$\sigma(W^{+}) + \sigma(W^{-}) \equiv \sigma = 3.\mathrm{x}10^{-32}, \text{ and } B(W\rightarrow\mu\nu) = 8\%.$$

Assuming an integrated luminosity of $10^{36}$ $cm^{-2}$ we expect 1200 $W^{\pm}$'s in the central (C) detector and 220 $W^{\pm}$'s into both the forward (F) and backward (B) detectors. The detection efficiency is taken to be 1/2 (1/6) in the C (F,B) region.

Figures 1 and 2 show the rates into the central detector. The shape of the muon spectrum as a function of $P_t$ has been taken from a Monte Carlo Model[4], and the result is shown in Fig. 1. The Jacobian peak shown in Fig. 2a will be somewhat washed out by the experimental momentum resolution as shown in figure 2b.

Figures 3 and 4 show the rates into the F,B detectors. In the central region the charge asymmetry of the W decays is too small to measure. In the F/B regions the asymmetry is sizable. Figures 3a and 4a show the $\mu^{+}$ and $\mu^{-}$ yields into the F detector, while Figures 3b and 4b show the asymmetry, defined as

$$A = \frac{N(\mu^{-}) - N(\mu^{+})}{N(\mu^{-}) + N(\mu^{+})}$$

For the expected yields of 150 $\mu^+$ and 70 $\mu^-$ in the F detector, A = 1/3.

Figure 4 shows the effect of resolution on the yield and asymmetry. Note that in the F/B regions there are two independent momentum measurements, one from the LAPDOG air toroid and one from the muon steel toroid. The two resolutions are comparable, and the net resolution is indicated by the horizontal bar in the figure.

The $Z^O$ cross section and muonic branching ratio are taken to be

$$\sigma(Z^O) = 10^{-32}\ \text{cm}^2, \text{ and } B(Z^O \to \mu^+\mu^-) = 3\%.$$

The detection efficiency into the combined F, C, B detectors is $\varepsilon(Z^O) = 1/2$. Using the usual ($10^{36}$) luminosity the yield is approximately 150 detected dimuon events. As discussed below (Multileptons), the major background is due to the decays of heavy flavors. Using the charge identification available from this detector we can estimate the heavy flavor backgrounds from like-sign dimuon and the trimuon rates.

In Fig. 5a is plotted the smearing of the $Z^O$ signal by the momentum resolution. While we are unable to measure the $Z^O$ width the total yield into dimuons is a useful check on the LAPDOG high resolution measurement of $\Gamma_{Z^o}$. As shown in Fig. 5b the 150 events are clearly detectable over the heavy quark background. Note that the background appears slightly larger than that in Fig. 8b. The increase is because here the momentum resolution has been folded in. This factor is roughly 1.7 at M = 40 GeV. Backgrounds other than from heavy quark decay are neglected. As will be discussed below, in the case of the single lepton spectrum, they are small. The expectation is that single lepton backgrounds will be more difficult than multilepton backgrounds.

## B. New Phenomena

Many other more exotic sources of leptons can be imagined. The muon detector together with the high resolution electron and photon capability of the LAPDOG detector will have no equal at seeing these events. New generations will yield multilieptons. Heavy leptons will yield Jacobian peaks from $L^{\pm}\rightarrow\mu^{\pm}\nu$ or mass peaks from $L^{0}\rightarrow\mu^{+}\mu^{-}$. Decays such as $M^{+}\rightarrow\mu^{+}\gamma$ or $W^{\pm}\rightarrow\mu^{\pm}\gamma$ have spectacular experimental signatures. In this speculative vein, the angular distribution $d\sigma/d\eta$ is shown in Fig. 6 for the production of very massive objects using the Bourquen-Gaillard phenomenological model. Clean muon detection at wide angles is crucial should such a heavy object be produced at the FNAL collider.

## C. Heavy Flavors

The study of heavy flavor production is an important physics goal in itself, but in the discussion of heavy boson detection the heavy flavor decays are a background source to be removed. We have two distinct but overlapping methods to isolate and map heavy flavor decays. One uses the topological information from the LAPDOG detector to select or veto events coming from jets. The other uses the charge information from the muon detector. The sequential decays from the jet events will be analyzed to study heavy flavor production and the like-sign dimuons and trimuons will be used to estimate backgrounds remaining in the heavy boson signal after the topological cuts have been applied.

In Fig. 7a is shown the expected cross sections for heavy quark pairs. Note that $\bar{b}b$ and $\bar{t}t$ production are copious on the scale of $W^{\pm}$ or $Z^{o}$ production. For branching ratios we take $B(c \rightarrow \mu^{+} \nu\ d) = 1/10$ and color counting is used to estimate $B(b \rightarrow \mu^{-} \nu\ c) = 1/6$ and $b(t \rightarrow b \mu^{+} \nu\ ) = 3/20$. Under these assumptions the like-sign and unlike- sign dimuon rates in Fig. 7b are derived. Substantial rates for dimuons are expected.

Table I shows the dimuon and trimuon branching ratios expected. $\bar{b}b$ is signalled by dimuons while $\bar{t}t$ is signalled by trimuons.

| TABLE I | | | | |
|---|---|---|---|---|
| Heavy Quarks | Final State Branching Ratio (Color Counting) | | | |
| | $\mu^+\mu^-$ | $\mu^\pm\mu^\pm$ | $\mu^+\mu^-\mu^\pm$ | $\mu^\pm\mu^\pm\mu^\pm$ |
| $\bar{c}c$ | 1/100 | 0 | 0 | 0 |
| $\bar{b}b$ | 1/14 | 1/30 | 1/90 | 0 |
| $\bar{t}t$ | 1/10 | 1/20 | 1/40 | 1/200 |

A crude estimate of the angular distribution of multilepton sources is shown in Fig. 8a. The F,C, and B detectors give good coverage of $Z^o$ and $\bar{t}t$ leptons while leptons from $\bar{b}b$ and $\bar{c}c$ extend to smaller angles. Integrating over angles, the yield of dimuons expected in a Monte Carlo model[5] is shown is Fig. 8b. Note that heavy flavor decays bury the Drell-Yan signal by large factors. Unless incisive topological cuts are available the Drell-Yan signal in general, and the J/ψ, T signals in particualr, are likely to be unobservable at the collider.

As shown in Fig. 8b, like-sign dimuons, indicating $\bar{b}b$ production are easily observable. Similarly, like-sign trimuons occur at observable rates, indicating $\bar{t}t$ production. Note that the invariant mass of these multileptons extends out to substantial values.

Topological cuts (isolation, missing $P_t$) will be used to separate heavy boson decays from heavy flavor decays. Like-sign dimuons and trimuons will be used to estimate the residual contamination in the heavy boson sample. The heavy flavor sample will be analyzed in its own right.

## D. Single Lepton Backgrounds

To evaluate backgrounds, the pion yield is taken from extrapolated data[7], and the muon yield from semileptonic decay of heavy flavors is taken from a model which has been fitted to all data[8]. Over the range of pseudorapidity ($\eta$) covered by this experiment the yield is assumed to be constant in $\eta$. All rates are quoted assuming an integrated luminosity of $10^{36}$ $cm^{-2}$.

Decay backgrounds are calculated taking a decay path from the collision point to $1\lambda$ into the LAPDOG detector. The rejection factor is $0.016/p$ for the central region and $0.054/p = 0.014/p_t$ for the F/B regions; these factors are roughly equal. The resulting decay background rates are shown in Fig. 9.

Heavy flavor backgrounds are taken directly from reference 8. A "top" mass of 20 $GeV/c^2$ is assumed in this model. For $p_t > 20$ GeV prompt muons from heavy quarks dominate the decay background in both the F/B and central regions. The Drell-Yan rate is ignored since it is dominated by muons from heavy quarks.

Also shown in Fig. 9 is the punch-through due to hadrons which do not interact. The rejection factors are 9000 in the central region and 49,000 in the F/B regions which are thicker. In both cases non-interacting punch-through is a minor source of background.

The question of interacting punch-through still needs to be adressed. Basically the question is "where is a shower punch-through in phase space?" The UA1 collaboration quotes large rejection factors on the basis of exit angle and position alone[9]. For example, at $p_t$ = 30 GeV/c the quoted rejection factors, scaled to our geometry, are $2.5\text{x}10^6$ in the central region and $5\text{x}10^7$ in the F/B regions. These factors are substantially larger than those for non-interacting punch-through. In addition, this experiment has constrained line-line momentum tracking in the central region, and an independent momentum measurement from LAPDOG in the F/B regions. Given these additional constraints on phase space we have ignored backgrounds due to interacting punch-through.

Given the steeply falling background the experimental resolution is important. An exponential yield,

$$N(p) = N_o e^{-b(p-p_o)}$$

when convoluted with a Gaussian resolution,

$$P(p,p') = \frac{1}{\sqrt{2\pi}} e^{-(p-p')^2/2\sigma^2}$$

gives an observed yield,

$$N(p')=N_o e^{-b(p'-p_o)} \; e^{b^2\sigma^2/2}$$

For example, at $p_t$ = 30 GeV the slope is b=0.2 $GeV^{-1}$. With a resolution $\delta p_t = \pm 0.2$ the rate in the central region is raised by a factor of 2.05. In the F/B regions the LAPDOG toroid has a resolution $\delta p_t/p_t = 0.005\ p_t$ while the steel toroid has a resolution $\delta p/p = 0.16$. At $p_t$ = 30 GeV/c, folding the resolutions in quadrature, the factor is only 1.25 in the F/B regions.

As seen above the major backgrounds are from decays of heavy quarks and high $p_t$ hadrons. Both sources presumably originate in high $p_t$ jets. This being the case we can use the energy flow pattern from both LAPDOG and our hadron calorimetry to remove many of these events on topological grounds. The rejection factors have been evaluated using the jet Monte Carlo program "ISAJET". There are basically two factors, one due to the fact that the muon is unaccompanied by other jet fragments (the "toward" factor), and the other due to the fact that the neutrino is unseen leading to missing $p_t$ (the "away" factor). At a $p_t$ of 30 GeV/c the toward factor is 1/16 and the away factor is 1/10. These factors are evaluated conservatively in that the central calorimentor information is not used. The resulting single lepton backgrounds after topological cuts are shown in Fig. 10.

## III. Description of Apparatus

### A. Design Criteria

An elevation view of one half of the detector is shown in Fig 11. The other half images what is shown in the figure. The central and Forward/Backward regions are very similar in design. Drift tubes before and after the magnetized absorber provide the trigger as well as track information. Vertex tracking for off-line analysis comes from LAPDOG's tracking chambers. Scintillation counters inserted in the iron sample shower energy deposition to provide calorimetry.

There are four basic design criteria:

1. The iron must be thick enough to absorb showers effectively.

2. $\int B.dl$ coupled with tracking granularity must provide momentum measurement errors smaller than multiple scattering up to 100 GeV/c.

3. The calorimetry must be sufficient to detect energy which might otherwise have been ascribed to an undetected neutrino.

4. Occupancy in any detector element must be low. Occupancy is defined to be the probability of a hit in a detector element per inclusive inelastic event. In calculating the occupancy a rapidity density $\frac{1}{\sigma}\frac{d\sigma}{d\eta}=3$ was used.[10]

The result from optimizing the design to meet these criteria is a detector with 1500 tons of magnetized steel instrumented by 300 phototubes and 13,000 drift tubes. Table II shows the main parameters (rapidity coverage, weight, number and occupancy of elements ) for each of the F, C, and B regions.

TABLE II

MAIN PARAMETERS OF DETECTORS

| Detector | $\Delta\eta$ | Weight (tons) | N Prop Tubes | Occupancy (%) | N Scint | Occupancy (%) |
|---|---|---|---|---|---|---|
| F, B | 1.6 | 220 | 4096 (5 cm) | 1.25 | 72 | 6.7 |
| C | 1.8 | 1100 | 4960 (10 cm) | 1.1 | 128 | 4.1 |
| Total | 5.0 | 1540 | 13152 | 1.2 | 272 | 6 |

B. Central Region Detector.

A view of the central detector is shown in Fig. 12. The core region contains the LAPDOG detector. It is surrounded by a layer of drift tubes followed by magnetized steel walls, each 120 cm thick. Following the steel are two more layers of drift tubes separated by 40 cm. These last two layers supply the exiting muon track vector. The tubes are 10 cm wide, which means a drift distance of 5 cm and a drift time of 1 μ sec. Each layer is a crossed xx'yy' assembly. Additional x,y tracking and stereo ambiguity resolution is supplied by the LAPDOG detector. Typical occupancy of these tubes is 1%.

Each of the four identical walls (top, left, right, bottom) is composed of six laminae of 20 cm thick steel. The laminae in each wall get wider and longer moving away from the beam, growing from 3.6 m wide by 5.4 m long to 5.6 wide by 8.4 m long. For each wall the construction is to build each lamina from two blocks of steel; both blocks are full length but only half the width of the lamina. For example, the eight blocks closest to the beam are each 1.8 m wide by 5.4 m long, and 20 cm thick. There are 48 blocks in all, 8 in each of the 6 concentric laminae.

Each of the 48 steel blocks is wound at the ends with wire to generate a very distorted toroidal field as shown in fig. 12. When the blocks are stacked the absorber has magnetic fields along the beam line; i.e., barrel stave fields. There are 8 staves (fields) covering the $2\pi$ azimuth. Four of them, one in the center of each wall, cover $2\pi/6$ each. The other four barrel stave fields are in the corners where the absorber walls meet, each covering $2\pi/12$. The eight fields alternate direction, the wall center fields going with the protons and the corner fields going with the antiprotons, or vice versa. The flux returns are outside the $\theta = 90^{\circ} \pm 45^{\circ}$ coverage of the central barrel.

Each lamina has 8 small gaps in its azimuthal coverage but by construction the gaps are aligned to point at the beam line so the loss in acceptance is negligible. The assumed field is only 14 kG to minimize fringe field leakage, power, and water cooling. The resulting 'barrel stave' magnetic field configuration is essential to confine the muon bending to the transverse plane so as to allow for a fast on-line momentum-threshold trigger. In the transverse plane the muon is constrained to come from a point (the beam line) whereas in a longitudinal plane the muon may originate anywhere is the 1 meter interaction region.

At present the calorimetry sampling is envisioned to be by scintillation counters placed after each of the first three 20 cm steel slabs. This corresponds to sampling at depths of $1\lambda$, $2\lambda$, $3\lambda$. There are 32 $\phi$ samples and 4 $\theta$ samples, leading to a typical occupancy of 4%. Both the scintillators and the drift tubes are divided in $\theta$ to decrease the occupancy. The tubes have two divisions in $\theta$ while the scintillators have four.

The active $2\lambda$ of the LAPDOG detector plus the $3\lambda$ of the steel calorimetry provide adequate depth. The resolution versus depth for a 30 GeV/c $p_t$ pion is shown in fig. 14a indicating that resolution does not improve beyond $5\lambda$. The steel shower sampling is rather coarse as indicated in Fig 14b where resolution versus thickness is shown. Nonetheless, for the purposes of topological cuts and improved hadron rejection for LAPDOG this resolution is sufficient.

## C. Forward/Backward Detectors

There are seven octagons of magnetized steel, each a 20 cm thick toroid having a 14 kG field. The added depth is required on the basis of desiring one punch-through hit per incident hadron at $p_t$ = 30 GeV/c[11]. The drift tube tracking is three layers of xx'yy' assemblies but the exiting muon layer arm has been increased to 60 cm because of the reduced multiple scattering at $p_t$ = 30 GeV/c ($p \simeq 110$ GeV/c). Tube width is reduced to 5 cm to preserve the 1% occupancy since particle density has increased. The slightly improved momentum resolution, folding in the LAPDOG air toroid measurement, is desirable for the delicate F/B muon asymmetry measurement.

The scintillator arrangement is shown in fig. 13. There are again three samples at depths of $1\lambda$, $2\lambda$, and $3\lambda$. The segmentation consists of 32 divisions in $\phi$ and two in $\theta$. All segments are roughly equal in rapidity. The average occupancy is 6.7% which is comparable to that of the central detector.

D. Summary of Apparatus

The occupancy for all tracking tubes is desired to be approximately 1%, and this, together with the requirement that resolution be better than multiple scattering, has dictated the cell size. The exiting muon lever arm has been set so that multiple scattering dominates measurement error for $p_t < 100$ GeV/c. The steel thickness is such that less than one punchthrough track per incident track exits for $p_t < 30$ GeV/c. This requirement ensures that non-interacting punchthrough is a minor background. The remaining interacting punchthrough can be removed using the 'Coulomb telescope' method of matching the entering and exiting track vectors. The calorimeter resolution is adequate for its purposes. In short, the apparatus is a superb muon detector providing crude but sufficient calorimetry.

## IV Trigger Rates

### Introduction

Triggers are generated by charged particles exiting the absorber and passing through the two tube layers. The background spectrum from $\pi$ and K decays and punchthrough has a steeply falling $p_t$ dependence, $dN/dp_t^2 \propto \exp(-bp_t)$ where b $\simeq$ 4. The absorber depth is such that less than one particle exits for each showering hadron incident at $p_t$ = 30 GeV/c, but for this discussion we are conservatively assuming one exiting particle for each incident particle with $p_t$ greater than the absorber cutoff. Even though the absorber cuts off 99% of the incident spectrum, the remaining 1% is still too much for the final trigger decision which needs to process the appropriate drift times (TDC's) in order to determine the precise $p_t$

To lower the rate we filter with a first-level trigger which uses tube hits (i.e., without drift times) to estimate the $p_t$. This first level is set to be fully efficient at $p_t$ = 10 GeV/c, and has decreasing pass-through down to $p_t$ = 3 GeV/c. It is particularly efficient at removing shower leakage particles which exit at wide angles. In estimating the rate into the second level we are again conservative in that we assume all particles above 3 GeV/c feed through the first level. Our concluding estimate of the rate into the second level is 21 Hz in agreement with the appropriately scaled measurement at UA1. The final trigger rate initiating readout of the detector can be set as low as desired by raising the threshold on the second level pass-through. The real trigger rate will have contributions from multimuons at lower thresholds and probably from triggers looking for e-μ events.

In the F/B regions the rates and trigger processing are similar to those in the central region. The absorber is thicker to contain the higher momentum hadron showers and the trigger rate is dominated by hadron decay into muons. The F/B trigger rate will be adjusted with the threshold on the first level trigger.

Calculation To estimate trigger rates we take a central density[10] of $1/\sigma . d\sigma/d\eta \simeq 3$, a luminosity of $10^{30}$ $cm^{-2}sec^{-1}$, and an inelastic cross section $\sigma_I$=50 mb. Multiplying these by $\Delta\eta = 1.8$ for the central detector gives the rate $R_C$ = 270 KHz. The absorber has a $p_t$ cutoff of 1.7 GeV/c. Cutting the spectrum $dN/dp_t \propto \exp(-bp_t)$ 1.7 GeV/c leaves $(bp_t + 1)\exp(-bp_t)$ = 0.9% for b = 4. The rate exiting the absorber is $R_C$ $(p_t > 1.7)$ = 2.3 KHz. Although the absorber depth leaks less than one particle per showering incident particle at $p_t$ = 30 GeV/c, we are here assuming one exiting particle per incident particle above $p_t$ = 1.7 Gev/c. The first level pass-through requires that the particle traverse pre-set "look-up" roads through the tubes. The tubes in each layer are staggered 10 cm cells so that the angular resolution is 5 cm. divided by 40 cm. To ensure full efficiency at $p_t$ = 10 GeV/c we set the road resolution at $p_t$ = 3 GeV/c. Assuming full efficiency at 3 GeV/c the rate to the second level is $R_C$ $(bp_t + 1)$ exp $(-bp_t)$ = 21 Hz. This rate is low enough to maintain a small deadtime from the second level.

Single muon trigger rates have been measured at the UA1 detector and have been found to be too high for the second level decision time. The present upgrade of that detector is adding 60 cm. of steel to the side walls and 40 cm. to the top. The estimate from UA1 for a luminosity of $10^{30}$ $cm^{-2}$ $sec^{-1}$ is 80 Hz. for 6 $\lambda$ absorber and 8 Hz. for 9 $\lambda$. The road resolution in the first level decision at UA1 is a little better because of the 60 cm. separation between the measuring stations. More information will be forthcoming soon from UA1 and we will use it to refine these estimates.

The trigger in this experiment is the appearance of a track behind the magnetized iron absorber. At this level a track is defined as a triple coincidence of hits in a road through the tubes. Because the muon originates at the beam line and bends in the transverse plane only, each road corresponds to a momentum window. The roads will be defined to accept $p_t$ = 10 GeV/c with full efficiency. The tube size then allows triggers from lower $p_t$ muons to leak through with decreasing efficiency down to $p_t$ = 3 GeV/c. This cut is sufficient to pace the slower second level trigger which reads the TDC's for the appropriate road and makes a precise calculation of $p_t$.

## V. Impact on Fermilab

The regions $25^{\circ}<\theta<45^{\circ}$ and $135<\theta<155^{\circ}$ are obviously holes in the detectors. Filling these regions must be considered in the context of a detailed engineering integration of P-714 and P-728 taking into account installation and maintenance requirements.

Detailed design may also succeed in reducing the transverse dimensions of the core detector. That would allow us to either increase our steel thickness or reduce the dimension of the required collision hall.

The total weight of steel is estimated at <u>1000</u> tons in the central detector and <u>500</u> in the F/B detectors. The volume of the apparatus is within the 750 $m^3$ guideline for the D0 area. A rough cost estimate is \$2 M for the experiment, of which the major portion is for the high quality steel necessary for the "building block" type of construction.

It is also clear to us that our muon detector requires larger collision and assembly halls than several other proposals or than for LAPDOG by itself. Of course, there are long range advantages to constructing a large D0 area now, rather than making a small one and having later to enlarge it. We feel that the physics we propose justifies the size area required. However, in an attempt to reduce the total financial impact on the U.S. high energy physics budget of the D0 civil construction plus detector we have started some preliminary inquiries into obtaining the steel blocks from outside the U.S.

We feel the same sorts of time pressures discussed by P-714 in their February 1 submission to the P.A.C.: competition from other accelerators, long lead time in designing and ordering the components of this large system, and design and construction of the D0 experimental area which cannot really start seriously until an experiment(s) is/are approved. Therefore we urge an early decision.

FIGURE CAPTIONS

1. Muon yield into the central detector. The background before and after topological cuts is shown for comparison. Rates assume an integrated luminosity of $10^{36}$ $cm^{-2}$.

2. $W^{\pm} \rightarrow \mu^{\pm}\nu$ yield into the central detector. Rates assume an integrated luminosity of $10^{36}$ $cm^{-2}$.

   (a) before resolution smearing

   (b) after resolution smearing

3. (a) $W^{\pm}$ yield into the F,B detector.

   (b) $W^{\pm}$ asymmetry in the F,B detector.

4. same as figure 3 but showing the effect of resolution smearing.

5. Yield of $Z^{o}$ events.

   (a) effect of momentum smearing on the mass spectrum

   (b) heavy quark backgrounds in the $Z^{o}$ region.

6. Angular distribution for production of very massive objects.

7. (a) The expected cross section for the production of heavy quark pairs.

   (b) The dimuon yield from heavy flavor decays as a function of quark mass.

8. (a) Angular distribution of various multilepton sources.

   (b) The dimuon yield as a function of dimuon mass from heavy flavor decays. The Drell-Yan signal is much smaller and shown for comparison.

9. Single lepton background rates.

   (a) into the central detector

   (b) into the forward or backward detector.

10. The sum of single lepton backgrounds before and after topological cuts.

    (a) into the central detector

    (b) into the forward or backward detector.

11. Elevation view of the experimental apparatus.

12. View of the central detector. Only 3 of the 4 identical sides are shown.

13. Cross section through the F,B detector showing the arrangements of scintillators.

14. (a) Resolution vs. depth for a 30 GeV/c muon.

    (b) Resolution vs. sampling thickness for a 30 GeV/c muon.

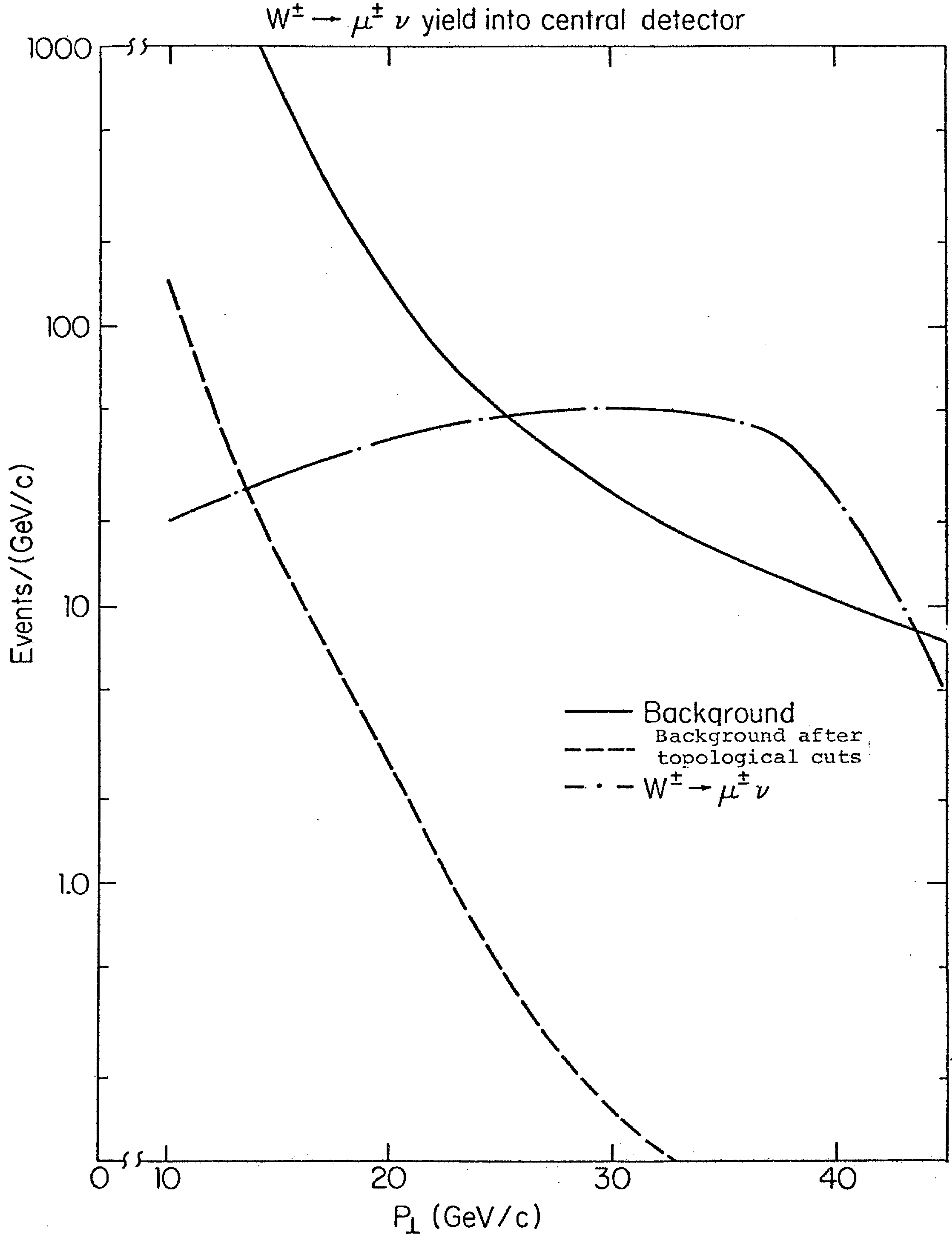
W± → μ± ν yield into central detector
1000
100
10
1.0
Events/(GeV/c)
0
10
20
30
40
P⊥ (GeV/c)
Background
Background after topological cuts
W± → μ± ν

Figure 1

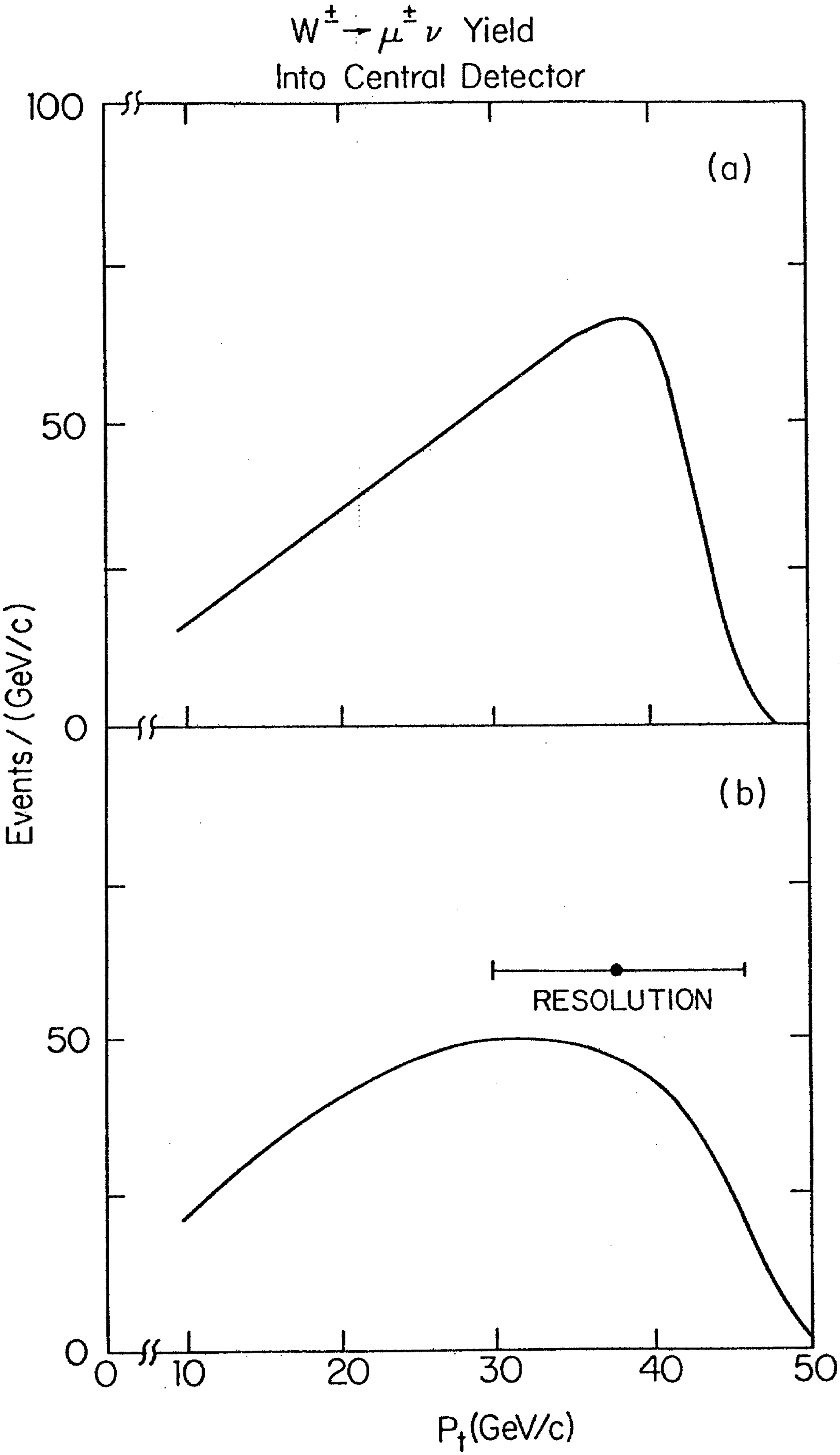
$W^{\pm} \to \mu^{\pm} \nu$ Yield
Into Central Detector
100
50
0
(a)
(b)
RESOLUTION
50
0
0
10
20
30
40
50
Events / (GeV/c)
$P_t$(GeV/c)

Figure 2

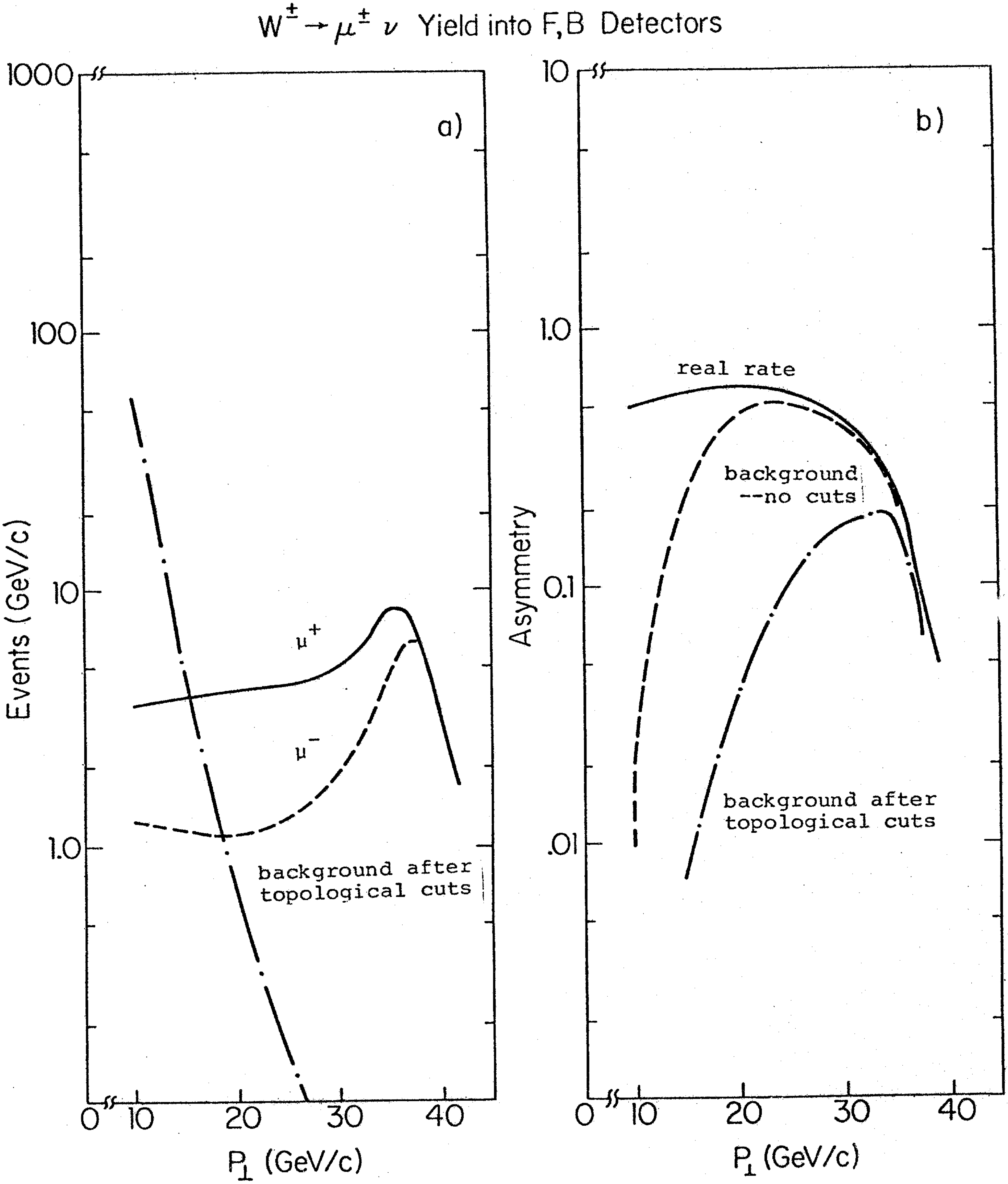
W± → μ± ν Yield into F,B Detectors
a)
1000
100
10
1.0
Events (GeV/c)
μ+
μ−
background after
topological cuts
0
10
20
30
40
P⊥ (GeV/c)
b)
10
1.0
0.1
.01
Asymmetry
real rate
background
--no cuts
background after
topological cuts
0
10
20
30
40
P⊥ (GeV/c)

Figure 3

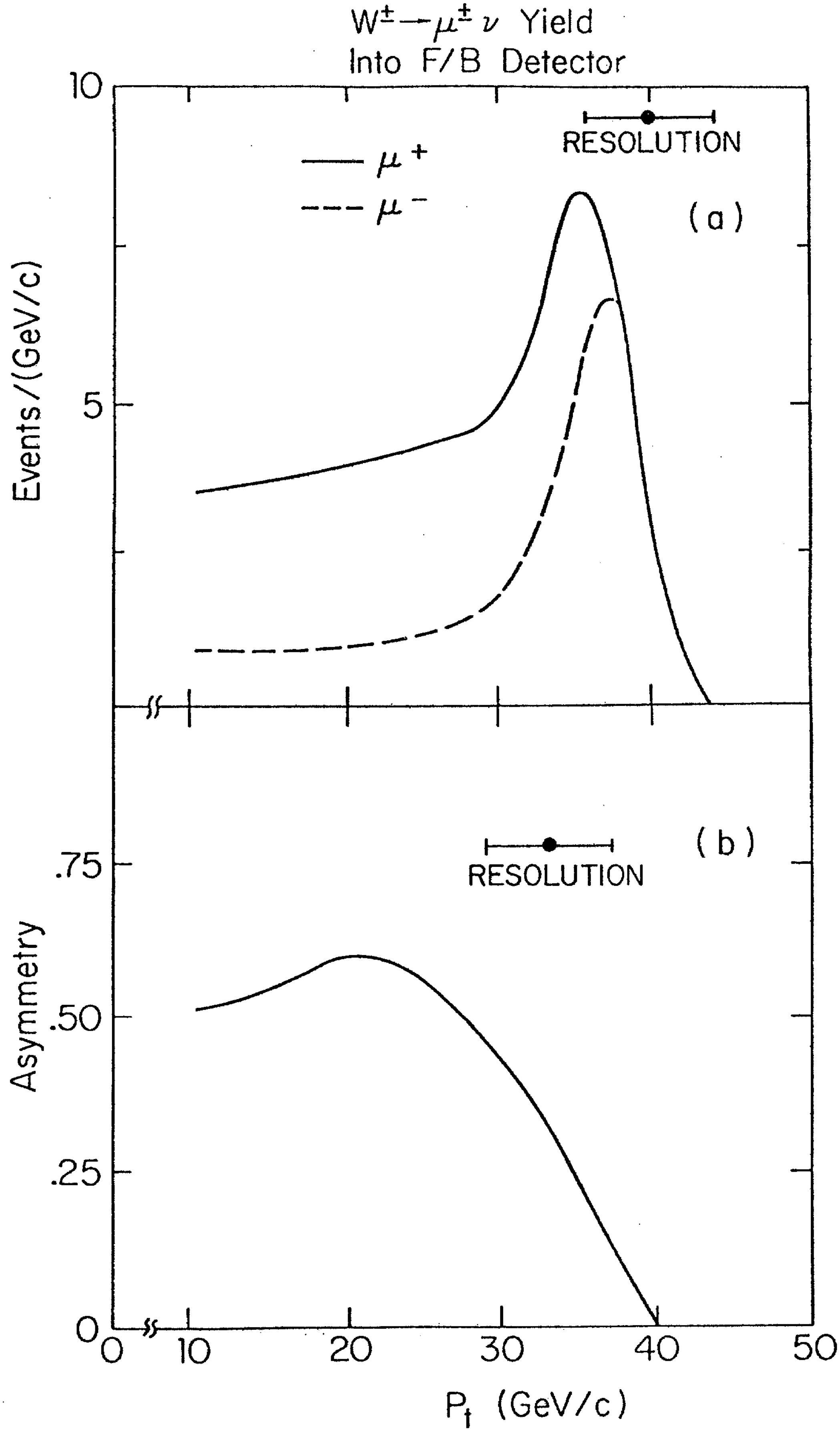
W± → μ± ν Yield
Into F/B Detector
10
5
0
.75
.50
.25
Events/(GeV/c)
Asymmetry
RESOLUTION
RESOLUTION
— μ+
--- μ−
(a)
(b)
0
10
20
30
40
50
Pt (GeV/c)

Figure 4

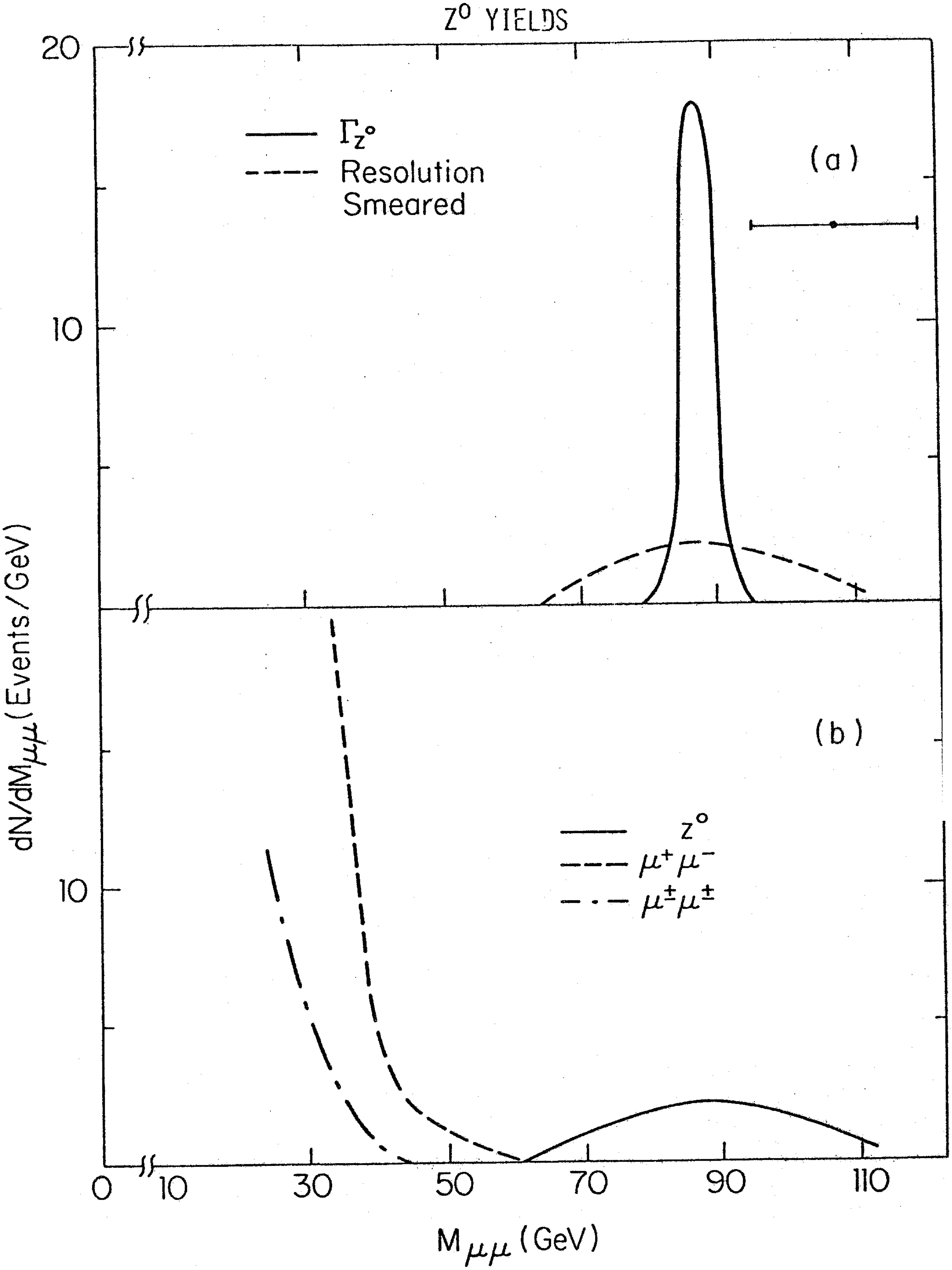
Z$^0$ YIELDS
20
10
$\Gamma_{Z^0}$
Resolution Smeared
(a)
(b)
Z$^0$
$\mu^+\mu^-$
$\mu^\pm\mu^\pm$
10
dN/dM$_{\mu\mu}$(Events / GeV)
0
10
30
50
70
90
110
M$_{\mu\mu}$ (GeV)

Figure 5

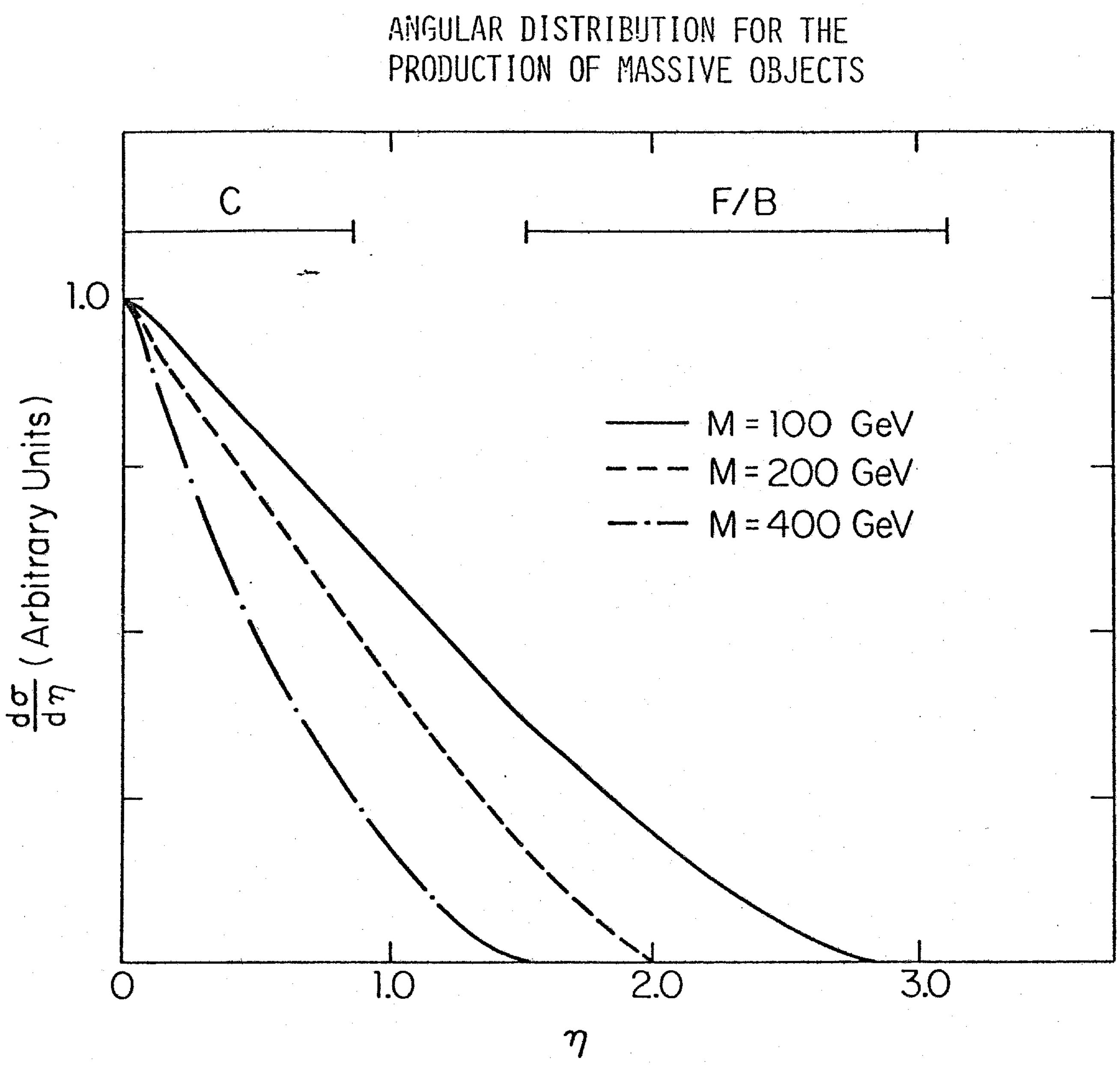
ANGULAR DISTRIBUTION FOR THE
PRODUCTION OF MASSIVE OBJECTS
C
F/B
1.0
M = 100 GeV
M = 200 GeV
M = 400 GeV
dσ/dη (Arbitrary Units)
0
1.0
2.0
3.0
η

Figure 6

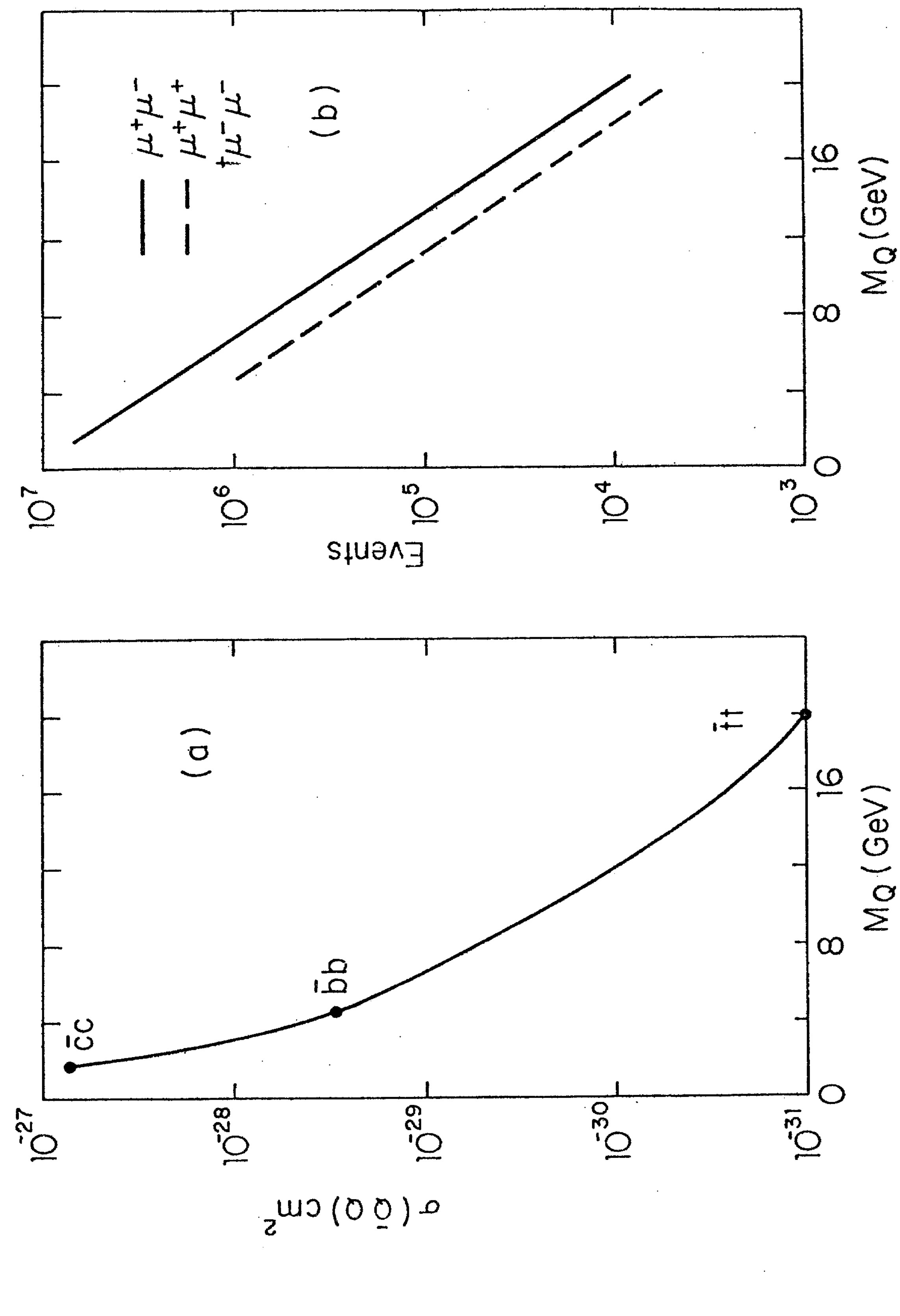
(a)
σ (Q̄ Q) cm²
10⁻²⁷
10⁻²⁸
10⁻²⁹
10⁻³⁰
10⁻³¹
c̄c
b̄b
t̄t
0
8
16
M_Q (GeV)
(b)
Events
10⁷
10⁶
10⁵
10⁴
10³
μ⁺μ⁻
μ⁺μ⁺
+μ⁻μ⁻
0
8
16
M_Q (GeV)

Figure 7

$$\frac{s - M_{\bar{Q}Q}^{2}}{2\sqrt{s}} = M_Q \sinh(\eta_{max})$$

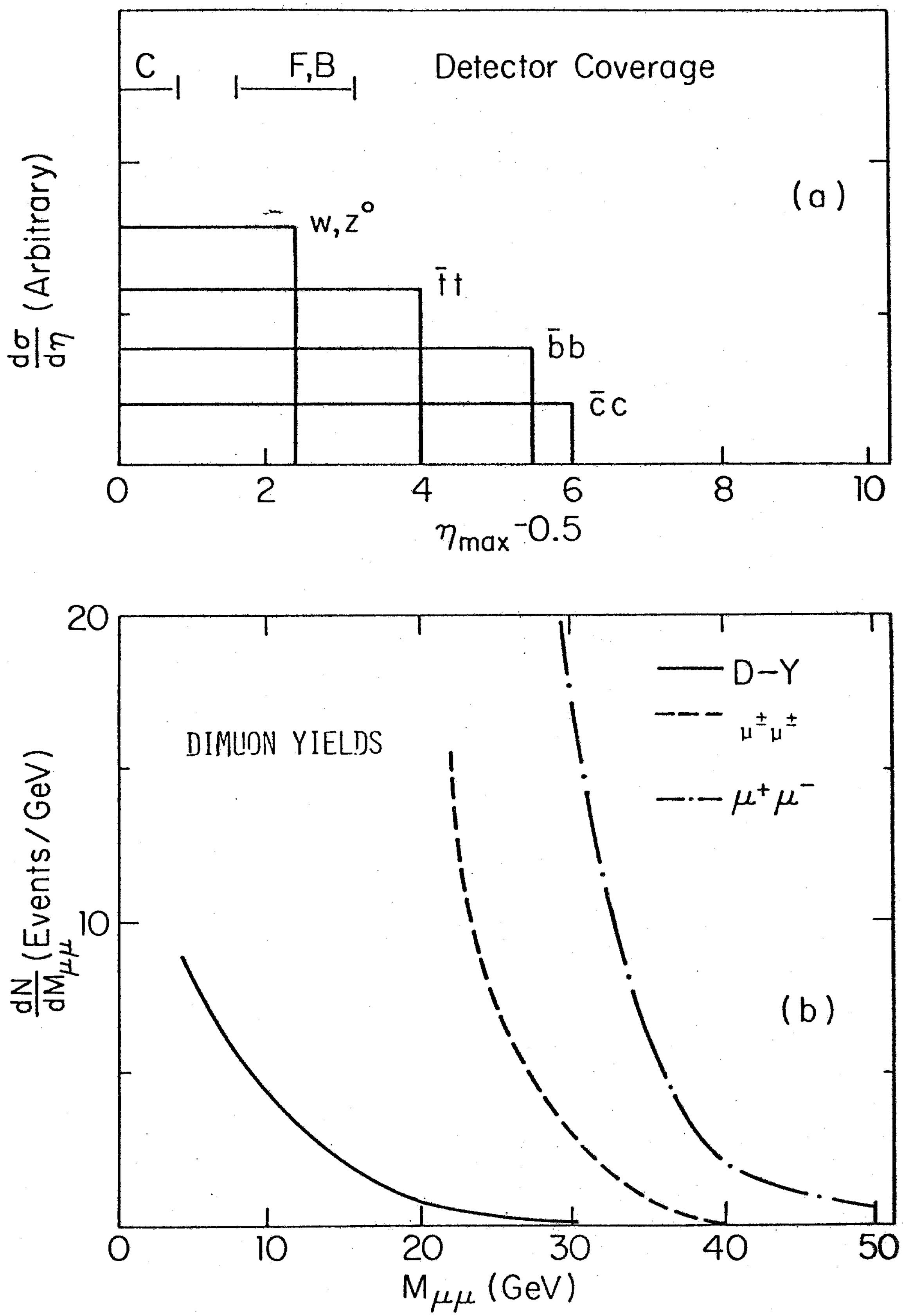


Figure 8

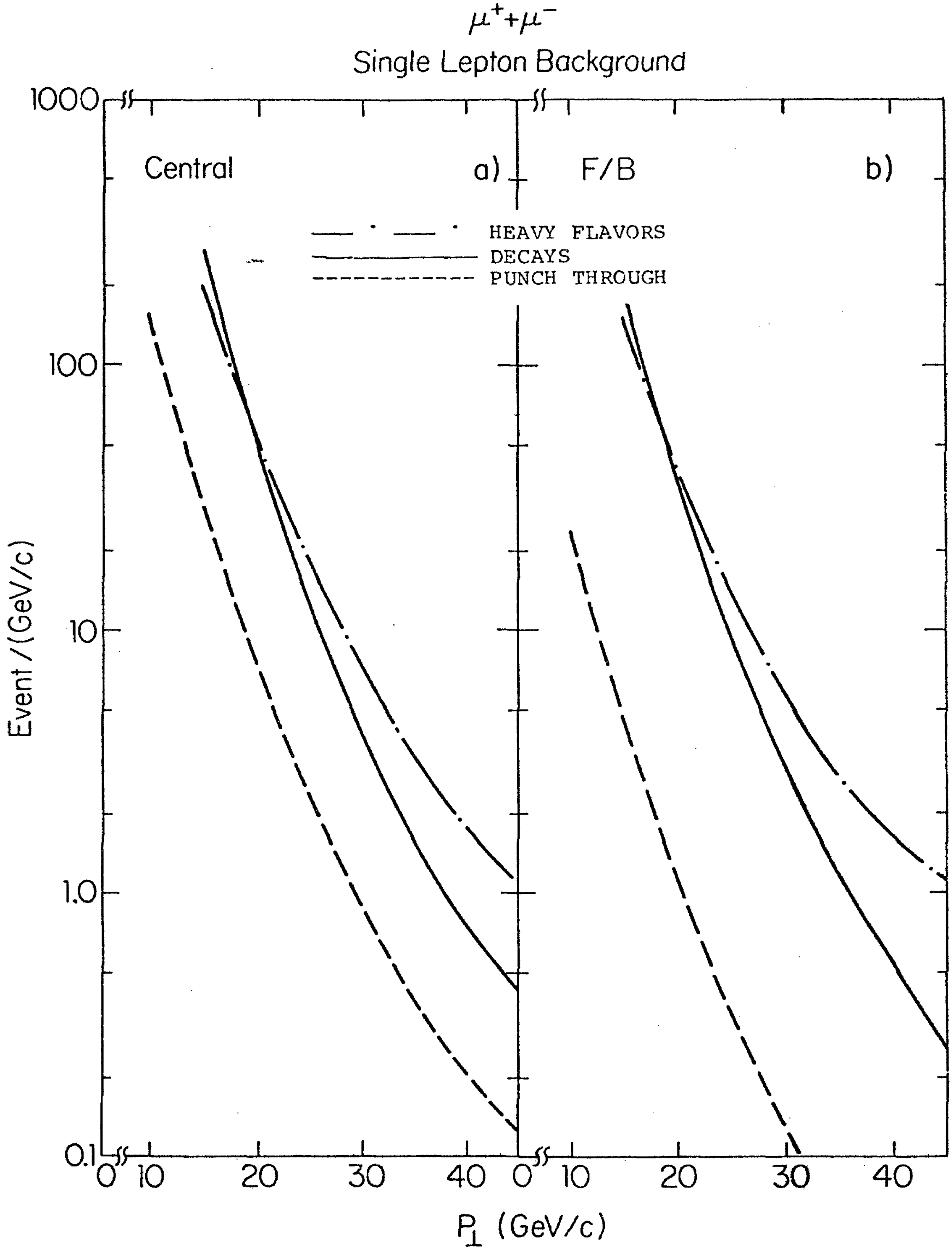
$\mu^+ + \mu^-$
Single Lepton Background
Central
a)
F/B
b)
HEAVY FLAVORS
DECAYS
PUNCH THROUGH
1000
100
10
1.0
0.1
Event /(GeV/c)
0
10
20
30
40
$P_\perp$ (GeV/c)

Figure 9

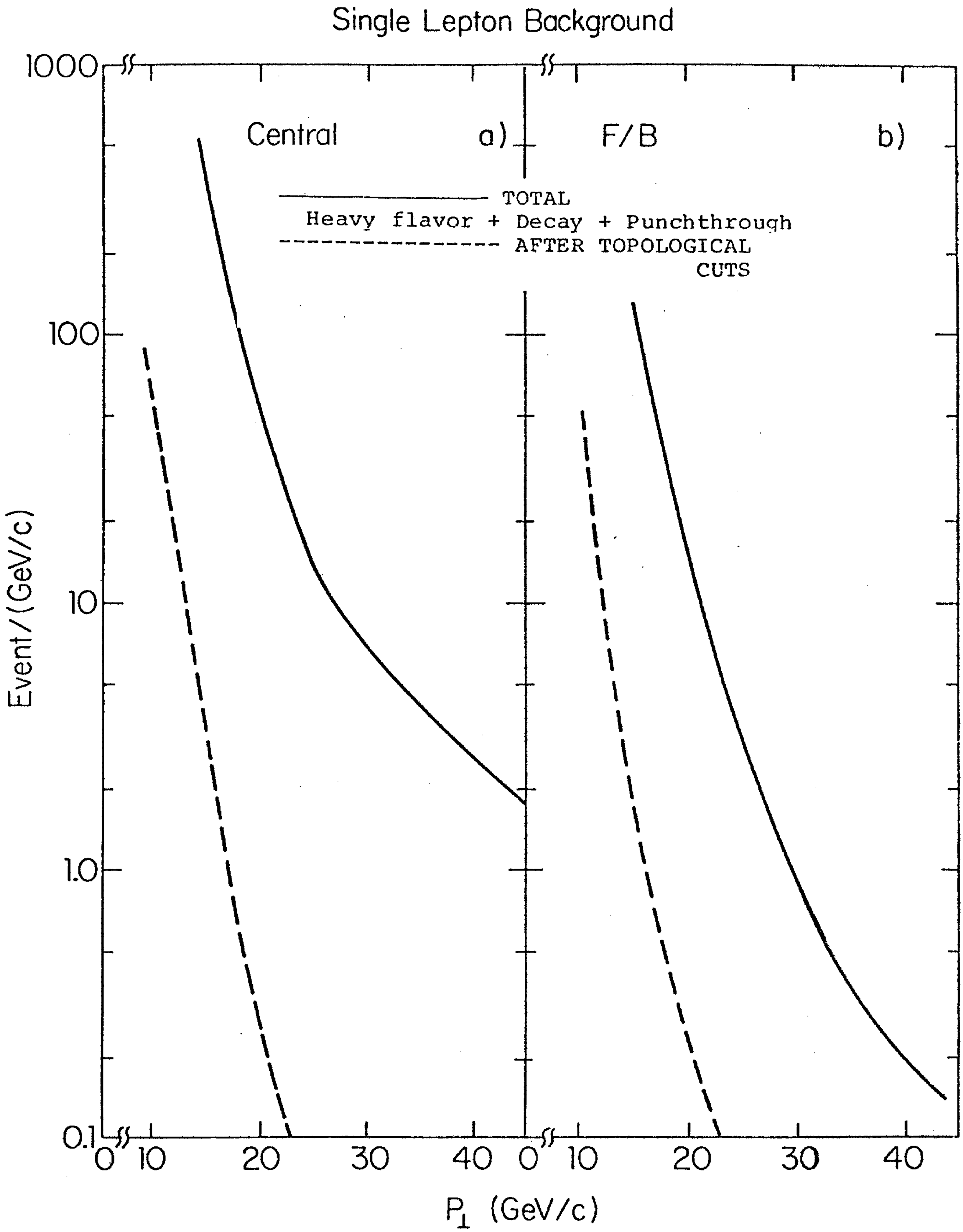
Single Lepton Background
1000
100
10
1.0
0.1
Event/(GeV/c)
Central
a)
F/B
b)
TOTAL
Heavy flavor + Decay + Punchthrough
AFTER TOPOLOGICAL CUTS
0
10
20
30
40
0
10
20
30
40
P⊥ (GeV/c)

Figure 10

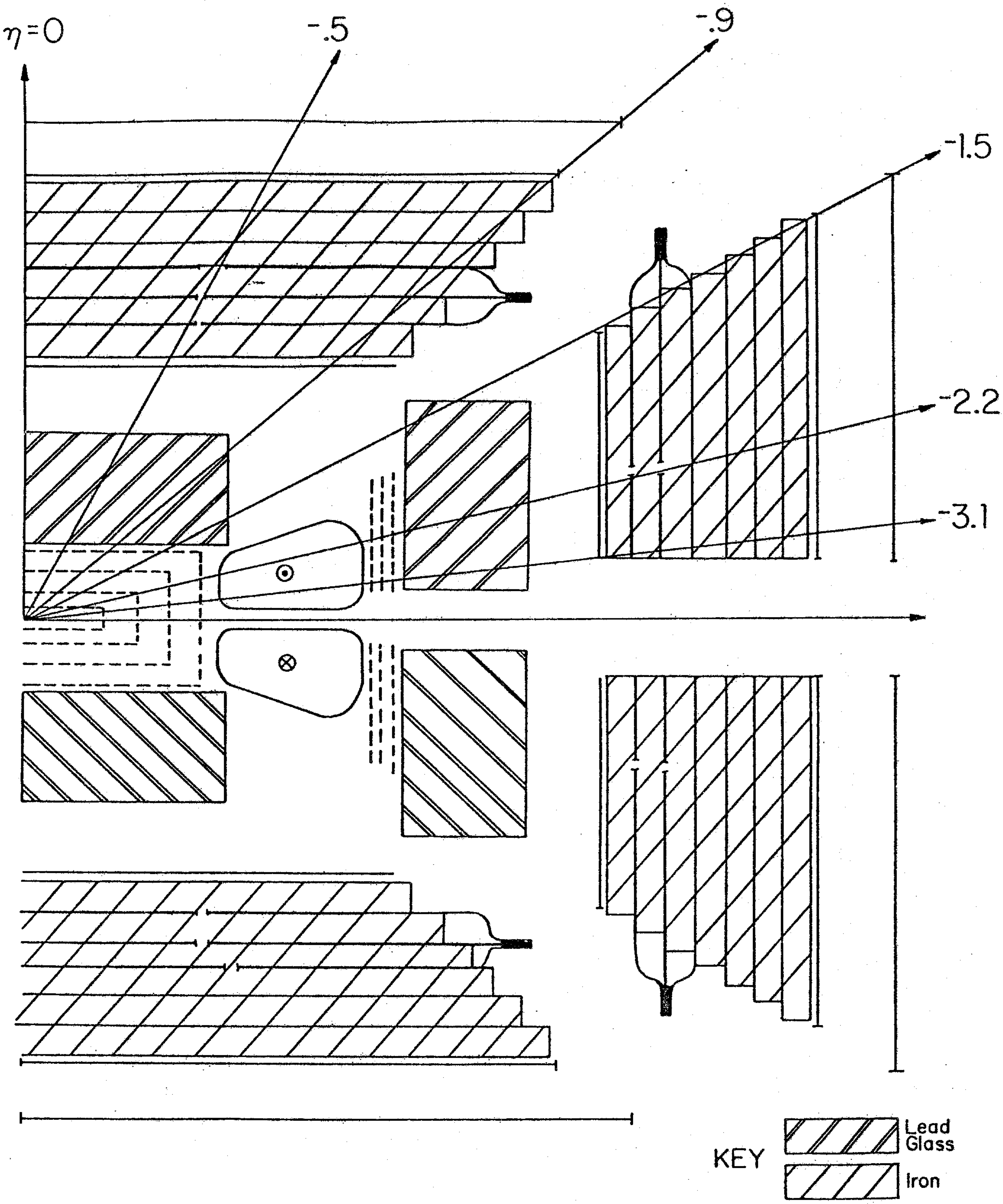


Figure 11

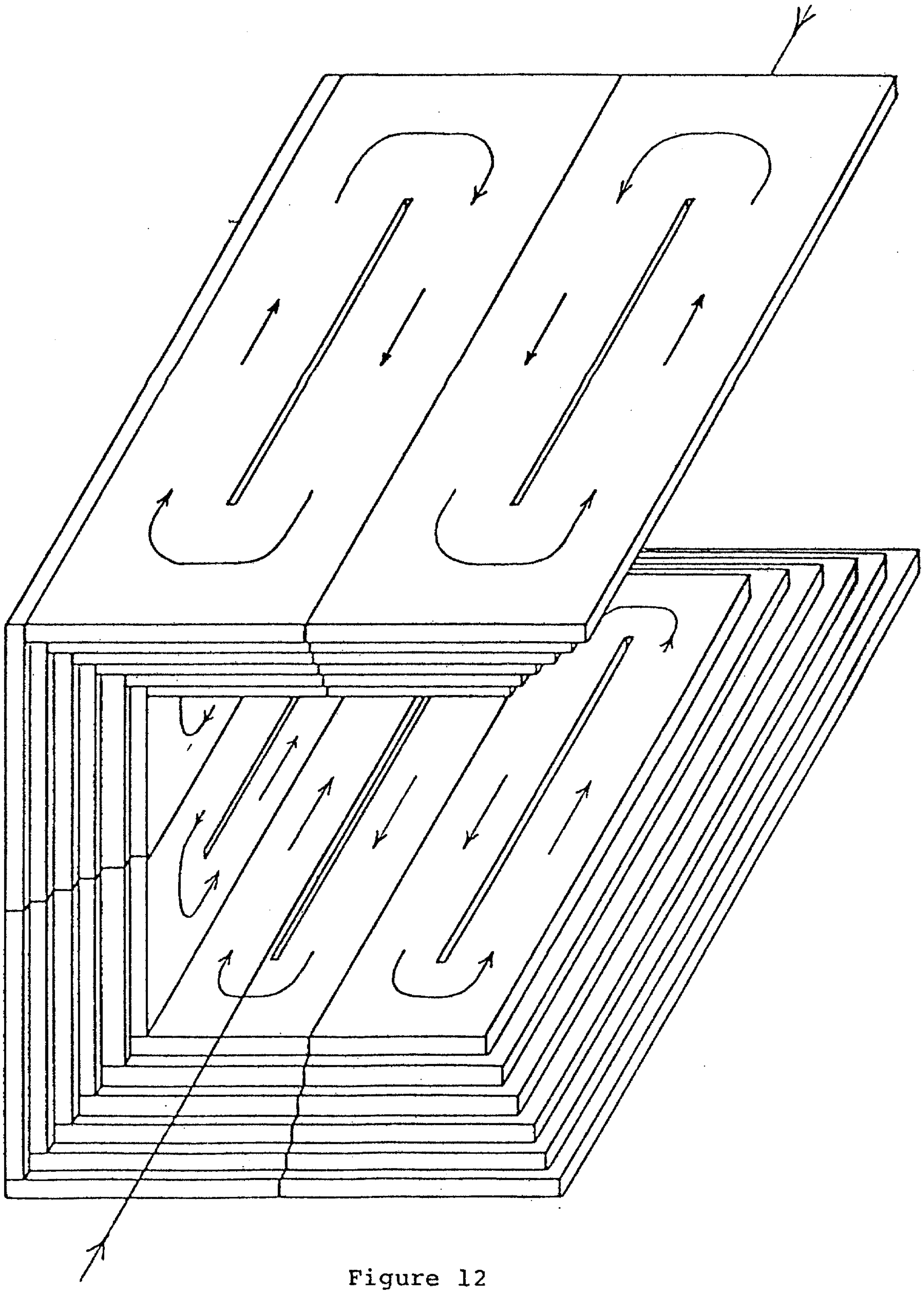

Figure 12

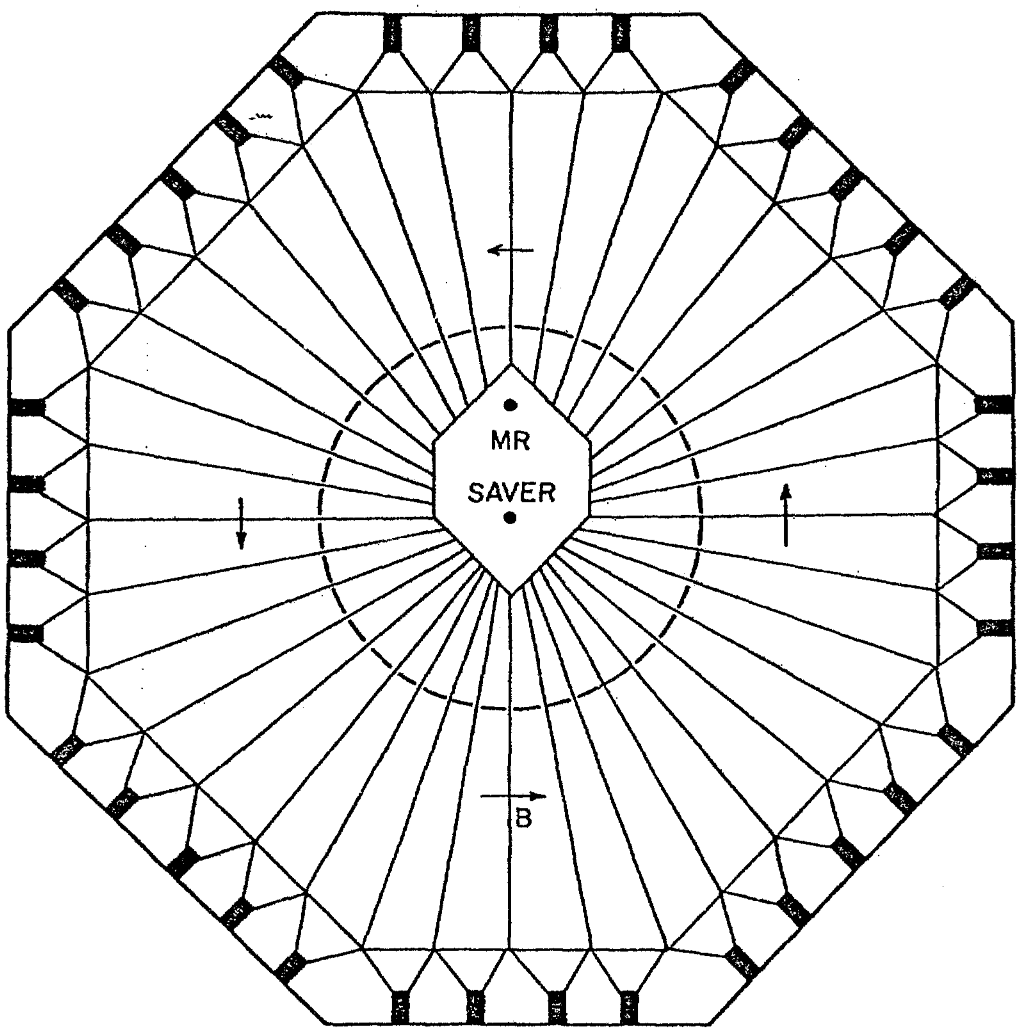


Figure 13

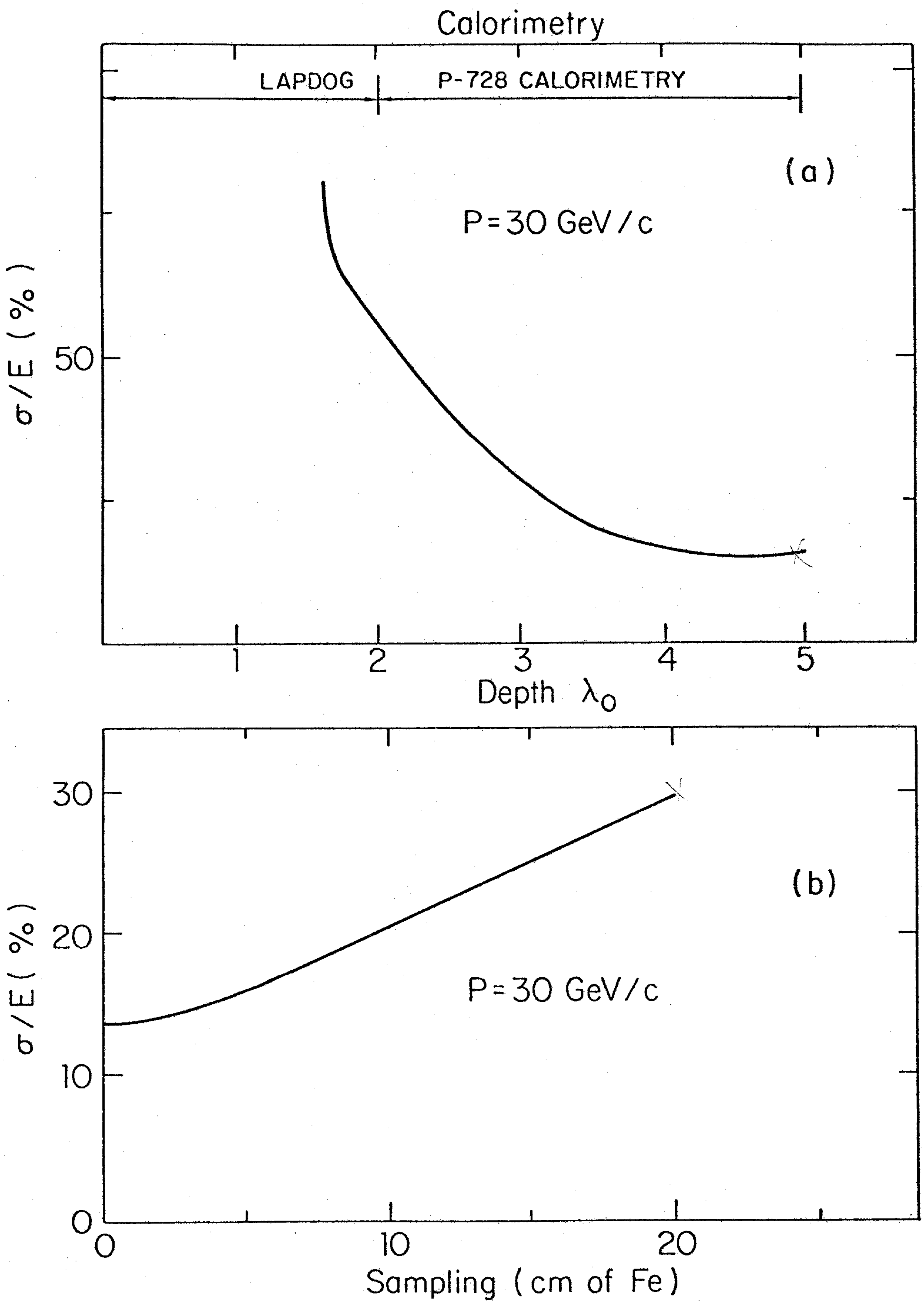
Calorimetry
LAPDOG
P-728 CALORIMETRY
(a)
P=30 GeV/c
σ/E (%)
50
1
2
3
4
5
Depth $\lambda_0$
30
(b)
20
P=30 GeV/c
σ/E (%)
10
0
0
10
20
Sampling (cm of Fe)

Figure 14

## References


1. Design Report for the Fermilab Collider Detector Facility (CDF) August, 1981

2. CERN/SPSC/82-51

3. F. E. Paige. BNL 27066.

4. F. E. Paige. BNL 30805.

5. e.g. F. Halzen, D. Scott, Wisconsin DOE-ER/00881-161 (1980).

6. F. E. Paige and S. D. Protopopescu. BNL-29777(1981)

7. R. Horgan, M. Jacob. CERN TH 2824 (1980).

8. F. E. Paige. A.I.P. Conference Proceedings no.85. p.168 (1981).

9. A. Astbury et. al. CERN/SPSC/78-19.

10. R. B. Meinke, A.I.P. Conference Proceedings no. 85. p.347 (1981).

11. S. Iwata. Tristan Workshop Review, DPNU-3-79.

Appendix A

**StonyBrook**

Department of Physics
State University of New York at Stony Brook
Stony Brook, NY 11794
telephone: (516) 246-6580

January 12, 1983

Dr. D. Green and
Dr. E. Malamud
Fermi National Accelerator Lab
P.O. Box 500
Batavia, IL 60510

Dear Dan and Ernie,

We have read with interest your letter of intent (P728) to upgrade the LAPDOG experiment by the addition of muon detection outside of our central detector.

We chose not to propose muon detection in LAPDOG because we felt that with the limited resources of a small (by comparison to CDF) collaboration, we should concentrate all of our efforts on doing a limited range of physics very well. Thus, our highest priority was, and still is, studying high transverse momentum electromagnetic particles with good spatial and energy resolution. With this in mind, we welcome your proposal to extend the physics that can be accomplished at D0, as long as we do not have to compromise our abilities to carry out our proposal.

We view your effort as a cost-effective way of doubling the available luminosity for the study of the leptonic decay modes of the vector bosons. Our examination of your proposal indicates that, in addition to extension of the physics program, your muon detectors will help us by providing needed shielding along the beam lines, and by enabling us to identify events with large missing $p_T$.

If the PAC approves both of our proposals, we would expect to cooperate closely with your group to ensure the successful execution of both experiments.

Sincerely,

Paul D. Grannis    Michael Marx
For the LAPDOG collaboration

MM;jd

# APPENDIX B

## MEASUREMENT OF MUON MOMENTUM

Muon Momenta will be measured using LAPDOG PWC's plus P-728 drift tubes to measure entrance angle and position. This will be followed by 1 meter of magnetized iron (14 kg.) and then 2 more stations of drift tubes to measure exit angle and position. The layout is shown in figure B.1. Note that in contrast with the layout drawings in the text, the steel immediately follows the lead glass. The amount of space, if any, between the lead glass and the steel will depend on the final design of the LAPDOG detector.

The proportional tubes are assumed to have a position resolution of $\pm$ 0.2 mm and thus, the exit angle is measured to $\pm$ 0.7 mrad. The resolution is dominated by the multiple scattering in the steel and is given by:

$$dp/p = 2ar/d \simeq \pm 0.18$$

where $d = B_o \, \mathrm{SQRT} \, (L_o \, \{3 + 4/(1+\delta)\} \, )$
and $a$=3335.6 kg.-cm.-GeV, $r$=14 MeV, $B_o$ = 14 kg., $L_o$ = radiation lengths of steel, $\delta$ = ratio of depth (in radiation lengths) of the lead glass to the steel.

The bend angle, multiple scattering angle, displacement, and multiple scattering displacement are shown in figure B.1. The ratio of 0.2 between multiple scattering and bend is not unreasonable. Also shown in the figure is the intrinsic error which is dominated by multiple scattering for momenta <100 GeV/c.

The above discussion has been for the C region. One can easily scale to the F/B region. In this region, $L_o$ is 1.5 m, $\ell_1$ is 60 cm., and $\sin\theta \simeq 0.26$. Thus $dp_t/p_t = dp/p = \pm 0.16$. Referring to the figure, the bend angles go down by a factor of $1.25\sin\theta = 0.325$, the multiple scattering angles go down by a factor SQRT(1.5)sinθ = 0.29, while the measurement error goes down by a factor 4/6 = 0.67. Rough scaling between the F/B and C regions has been maintained except for the measurement error. However, in the F/B region measurements will be augmented by using the LAPDOG tracking chambers.

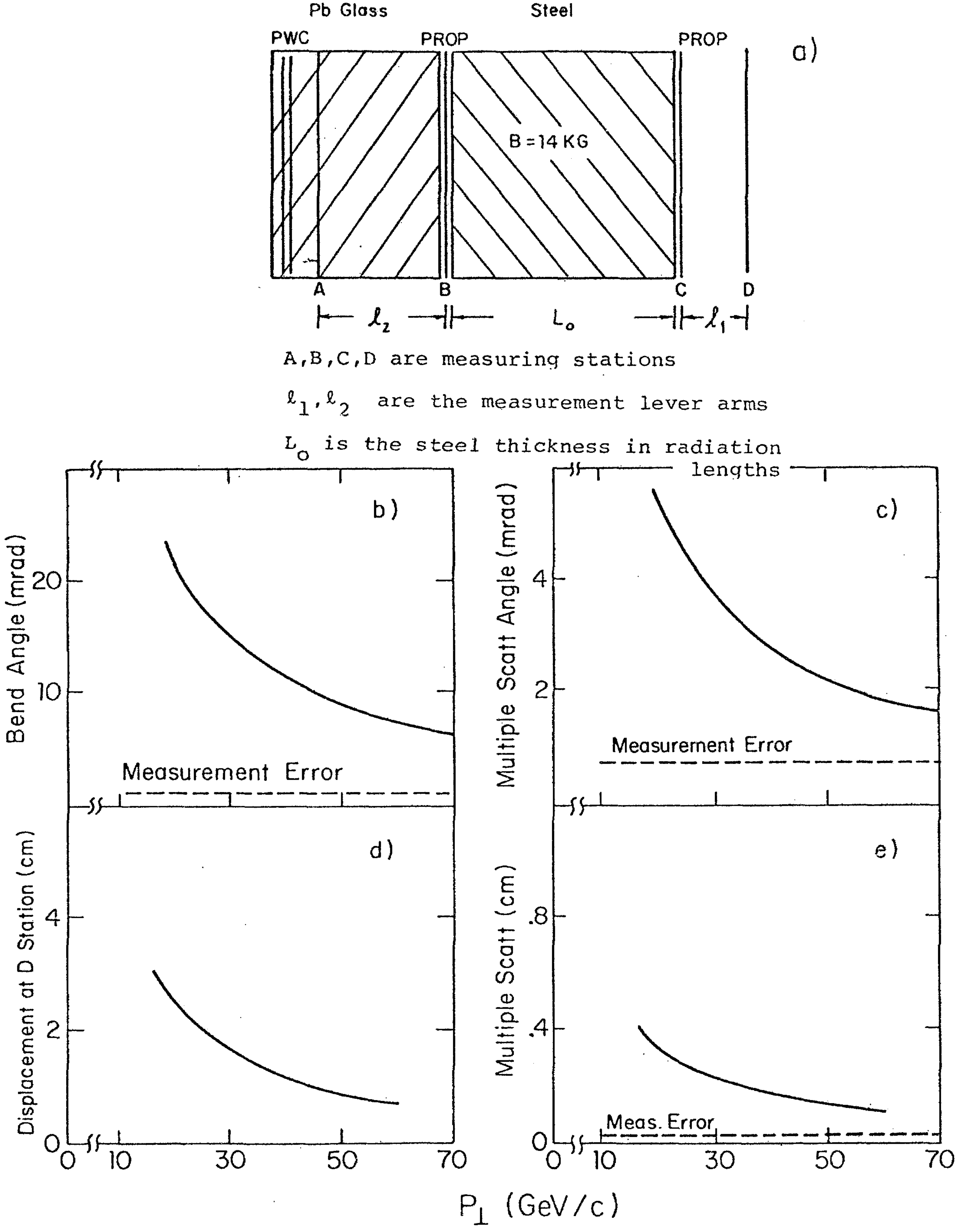
Pb Glass
Steel
PWC
PROP
PROP
a)
B = 14 KG
A
B
C
D
$\ell_2$
$L_o$
$\ell_1$
A,B,C,D are measuring stations
$\ell_1, \ell_2$ are the measurement lever arms
$L_o$ is the steel thickness in radiation lengths
b)
Bend Angle (mrad)
20
10
Measurement Error
c)
Multiple Scatt Angle (mrad)
4
2
Measurement Error
d)
Displacement at D Station (cm)
4
2
0
e)
Multiple Scatt (cm)
.8
.4
0
Meas. Error
0
10
30
50
70
0
10
30
50
70
$P_\perp$ (GeV/c)

Figure B.1

Fermilab Proposal No. P-712

Spokesperson: P. Rapp

Phone: (312) 840-4107

FTS 370-4107

# STUDY OF MUONS FROM $\bar{p}p$ COLLISIONS UP TO $\sqrt{s}$ = 2 TeV

I. Revisions to the original proposal (2/1/82).

II. Response to the PAC concerns (4/6/82).

May 18, 1982

Abstract We propose to measure the production of muons from the FNAL collider as a function of $\sqrt{s}$ and $p_t$. At low luminosity we can use the varying absorber length to separate and measure pion and prompt muon production. This beam dump mode allows us to measure the backgrounds leading into the electroweak boson region, a feature not available to either CDF or P-714 ("LAPDOG"). Our detector measures like-sign dimuons, a powerful handle on backgrounds unavailable to LAPDOG. Most important, our background from punch-through and pi-decay is a factor 15 below that for CDF, allowing any muon signal to be that much more cleanly seen. This will be especially important if the pion background is larger than expected or if the production of heavy masses is more momentum-smeared than expected. Total cost of the experiment, including low-beta quads and construction of the D0 area, is less than 10% of the cost estimated for CDF.

This letter contains two parts:

I Changes since P-712 was submitted

II Response to the PAC concerns (letter of 4-6-82.)

In section II we concentrate especially on demonstrating the unique physics capabilities of our apparatus relative to CDF.

I Changes and impact of changes

(a) Additional Collaborators. The collaboration has been broadened to include more University participation. The list now includes:

University of Arizona: Burt Pifer

George Mason University: Bob Ellsworth

University of Maryland: Pat Rapp (Spokesperson)

Virginia Tech: John Ficenec

Fermilab: D. Green, H. Haggerty, E. Malamud

(b) Increased acceptance. We have dropped the idea of trying to share the large angle region with another group. Both experiments in such an arrangement are compromised and a better solution is to run them in different years. Better physics is done by enlarging our apparatus to cover, for large polar angles, full 2-pi azimuth. The revised geometry is shown in Figure 1a,b,c.

(c) Field direction. As seen in Fig. 1 the field direction is now rotated $90^{\circ}$ from our original proposal. Although we could still design a magnet with the original orientation, once we go to 2-pi geometry a toroidal magnet has a particularly simple mechanical solution.

(d) Weight. The steel is now increased from 530 tons to 964 tons. In this new geometry all the steel is efficiently used for momentum analysis and ranging. At the core of the detector, inside the radius of the main ring, is 15 tons of copper (Fig. 1). This copper core is an efficient non-magnetic pion absorber and thus minimizes the magnetic field gradient across the main ring. We can do even better if tungsten or heavimet can be obtained.

(e) Triggering. The aboveground liquid scintillators are eliminated, leaving the detector completely underground and with left/right/up/down symmetry. $p_{min}$ is kept large by substituting the central copper for the external dirt. Cosmic ray triggering is minimized by dividing the non-bend projection into 32 triple-coincidence triggers. (Fig. 2) Each trigger telescope points at the beam line. Off-line, cosmic events are removed using the full-azimuth tracking. Up-down timing from the outermost scintillator counters is used also to reject cosmic background to the dimuon spectrum.

(f) Tracking. There are now three tracking stations, each covering full 2-pi azimuth. (Fig. 1) Each station has 10 layers of drift tubes (Fig. 3) and yields a track vector accurate to $\pm$ 1mr. These three vectors yield essentially two independent measurements of the momentum. They also provide a very tight 'Coulomb telescope' on a multiply-scattering muon, serving to distinguish the muon from candidate trajectories derived from a particle cascade.

(g) Magnet power. The magnets are excited to 15 kg with 140 turns and 100 amps. Power is 10 kw. Water cooling is not needed. The magnets will not be driven into saturation, since fringe field at the main ring beam location is critical.

(h) Stray field problem. Both the Main Ring and Doubler beam pipes pass through field free regions. Since the steel is not saturated we do not anticipate difficulty in shielding these pipes. We think the magnet can be on while the Main Ring is running. But, of course, we have to convince ourselves and the Accelerator Division of this. A rough estimate of the unshielded field and field gradients in the region of the Main Ring pipe are a few gauss and a few tenths of a gauss/cm. We feel that these fields are small enough to shield. All steel plates will be machined so as to keep field leakage into air gaps at a minimum.

(i) Assembly and Testing. The low power requirement makes it easy to assemble the complete magnet in an industrial building and measure the stray fields in the region of the beams. This will also enable us to work out and rehearse an efficient installation scenario.

(j) Installation. No caissons are needed. A "garage" for assembly is useful but not necessary if an overhead crane (capacity $\gtrsim$ 20 tons) is available. After assembly the region above our experiment would be plugged with concrete blocks and/or backfilled with dirt. A rough estimate, to be refined later, is that installation could be done in 20 working days (2 shifts/day).

(k) Size of area. Our apparatus is a cube 20' on a side. This cube gives us $\pm$ 45 $^{\circ}$ coverage in polar angle, 2-pi azimuthal coverage, and thickness on all sides of 12.6 absorption lengths, minimum. $P_{min}$ is 2.5 Gev/c for muons at normal incidence to the copper and is larger for muons at slant incidence. We feel, as discussed in Section IIe that punch-through is potentially a severe enough problem that this thickness is necessary. Because the detector occupys only 20' along the beam, only a few beam elements need to be rearranged when converting back to fixed-target operation (D0 extraction). It is possible that removal of the central copper, leaving a space 40" x 40" centered on the Saver pipe, would allow fixed-target operation with the steel remaining in place for the next collider running.

(1) Costs. The total cost is estimated at \$1150K, which breaks down into \$700K for the magnet, \$24K for the copper core, and \$425K for the detectors and associated electronics (4160 drift cells, 2134 $ft^2$ of NE102 scintillator, 160 phototubes, 4320 ADC's, and 160 TDC's). We note that even at full price, and including \$4M for the low-beta quads and the D0 area, the total cost is less than 10% of the \$60M estimated for CDF.

II Response to Questions

(a) Unique Physics capabilities relative to CDF. Clearly both CDF and P-712 propose to study final state muons. The main thrust of P-712 is that CDF is designed around tracking and calorimetry and, as such, makes some compromises with muon physics. We assert that in two crucial aspects, pion and kaon decay to muons and hadronic punch-through, P-712 will do a superior job. As explained in detail below, we find that our background due to these sources is a factor 15 below that for CDF. (Fig. 5) The pion source spectrum used is the same used by CDF[1].

(b) Luminosity Requirements. Naturally, any experiment designed to study electroweak physics requires high luminosity. Thus eventually, like most other users in the DO area we will request a low-beta insertion of reasonable strength, e.g. beta of 3 - 4 meters. Under initial low luminosity running conditions interesting physics can be extracted from P-712. For example, the mu $\pm$ yield due to heavy flavor production falls many orders of magnitude between our 2.5 GeV/c $p_t$ cutoff and the electroweak regime ($p_t \sim 40$ GeV/c). This is shown in Fig. 4. The yield from pi-decays and punch-through displays similar behavior. By utilizing the varying path lengths through the detector, by making minor changes in the decay path, and by measuring same sign and opposite sign dimuons, we will be able to separately extract the yield of pi $\pm$ as a function of $p_t$, and the yield of prompt muons vs. $p_t$. In this respect P-712 is basically a beam dump experiment. This "moderate" $p_t$ physics, $3 < p_t < 10$ GeV/c is interesting in itself and will serve as a prelude to electroweak physics. Note that the thin CDF detector necessitates a trigger $p_t$ cutoff $\gtrsim 10$ GeV/c which precludes that CDF study this sort of physics.

(c) Solid angle acceptance. As already discussed we have increased the azimuthal coverage to 2-pi. This results in a $W^+$ efficiency of 50% and a $Z^o$ efficiency of 33%. In rapidity we cover 2.0 units, compared to 2.2 for the central detector of CDF.

(d) (1) Background from pi-decay. We believe that the problem of pion decays has been optimized in P-712. The relevant scale factor is the available decay path, equal to the distance in air plus one lambda of absorber. For our detector this number is 20 cm. In comparison, CDF uses a conservative figure of 180 cm for the total decay path. This means that P-712 is lower by a factor of 9 in pi-decays, equivalent to a factor of 2 in momentum. This factor may be crucial if the Jacobian peak is not as pronounced as indicated in the model used by the CDF group. The question of the Jacobian peak will be discussed below in Section IIf.

(d) (2) Background from heavy flavor decay. If the top quark has a mass of 20 GeV, then the expected background has a magnitude and shape rather like that indicated in Fig. 4 for pi-mu decay. Again, by using varying path lengths through the absorber, we can separate the prompt muon yield from the pi-decay yield.

We emphasize the fact that P-712 measures charge, and therefore can use like-sign dimuons to get a handle on background sources. This capability is, for example, not available to P-714 ("LAPDOG"). We assert that, using like-sign dimuons, we can reduce the heavy flavor background, at least in a statistical and model dependent fashion, below that due to pi-decays. The like and unlike-sign dimuon background shapes with respect to the Drell-Yan and $Z^o$ signal are shown in Fig. 5 as an example.

(e) Punch-through. We feel that a great strength of P-712 with respect to CDF is in the problem of hadronic punch-through. Basically CDF has a thin absorber, 6.4 lambda, while P-712 has a thick absorber, 12.6 lambda. This means that the probability per hadron to pass through the absorber without interacting is 500 times worse for CDF.

Because we do not sample the energy deposition of the muon as does CDF, we have a background from showering punch-through in addition to the background from non-showering punch-through. To remove this shower background we use the "Coulomb telescope" described in Ref. 2 (Fig. 7). We have conservatively estimated our rejection by taking the square root of Rubbia's rejection factors (F in Fig. 7b), assuming only a one-dimensional telescope in our non-bend plane. In reality we expect the rejection to be much better since on each candidate track we have three vectors which must yield trajectory uncertainties consistent with the multiple scattering of a muon having the calculated momentum. Monte Carlo studies are necessary to determine accurate rejection factors. Our conservative estimation yields a showering punch-through signal equal to a few times the non-showering punch-through signal. In sum, our better rejection of the substantial punch-through background is one reason that P-712 is superior for doing muon physics.

Along this line we note that rejection by sampling kills any muon accompanied by a nearby showering particle. This may be risky.[2]

(f) Momentum Resolution The weakest point of P-712 is momentum resolution. Our stated momentum resolution of $\sigma/p = \pm\ 14\%$ is a compromise between our analytic calculation, confirmed by Monte Carlo, and the scaled results from Mark J and Ting's ISR dimuon experiment. Our calculation gives $\pm$ 12.8%, using a field of 15 kg and a spatial resolution of $\pm$ 200 microns.

Scaling by magnetic field strength and the square root of the path length we get $\pm$ 20.5% from Mark J, which sampled the track with vector, point, vector, and $\pm$ 16.7% from the ISR experiment, which sampled using 3 or 4 points and a vector. Our track sampling (vector, vector, vector) is shown by analytic calculation to be more accurate than either of these other methods. In essence we have two independent momentum measurements. Scaling the two reported results by accuracy of track sampling gives resolutions around ± 15%. Using our calculation and the two scaled estimates we have settled on ± 14% as our present best estimate. The resultant smearing of the W peak is graphed in Fig. 8.

We feel that punch-through and decay are problems of sufficient gravity that we choose to compromise on momentum resolution. Using the CDF model of W production, P-712 can easily see the Jacobian Peak (with delta-$p_t/p_t$ = ± 0.08) because we have reduced the punch-through and decay backgrounds. For CDF the thin absorber far from the interaction implies a poor peak to background ratio (Fig. 9). We note that many QCD models have a more badly smeared peak due to gluon radiation. If this be true, then background rejection is much more important than momentum resolution. An example due to Paige[3] is indicated in Fig. 6.

We hope that this response adequately addresses the concerns expressed by the PAC. We would be very happy to discuss any of these points in more detail with any member of the PAC.

## References

1.) I. Hinchliffe and R. L. Kelly, LBL-12274, CDF-83, Photon and Pi-zero Production at the FNAL Collider, February, 1981.

See also Design Report for the Fermilab Collider Detector Facility (CDF), August, 1981, Fig. 1.17.

2.) Proposal for a 4*pi Solid Angle Detector for the SPS Used as a $\bar{p}p$ Collider at a Centre of Mass Energy of 540 Gev, CERN/SPSC/78-06, SPSC/P92, January, 1978.

3.) F. Paige, BNL-30805, Monte Carlo Simulation of Heavy Quark Production in pp and $\bar{p}p$ Reactions, January, 1982.

See also F. Halzen, A. D. Martin, D. M. Scott, MAD/PH/41, DAMTP82/5, Does Large Transverse Hadronic Energy Accompany Drell-Yan Photons and Weak Bosons?, March, 1982.

## Figure Captions

1. Three views of the revised detector. Note that the absorber length is a minimum of 18" Cu plus 64" Fe, a total of 12.6 lambda.

2. Schematic of the 32 triple-coincidence scintillator telescopes used to trigger on muons. The telescopes point to the interaction region (width approximately 2 mm.) in the non-bend plane. They are instrumental in lowering the cosmic ray triggering rate.

3. A cutaway of one of the 3 full-azimuth triggering and tracking stations shown in Fig. 1. Each station consists of overlapped triggering scintillator counters and 10 layers of drift cells. Each station provides a vector accurate to ± 1 mr. in either projection. The three vectors on each track give accurate momentum determination and constrain muon candidates to a tight "Coulomb telescope", allowing near-elimination of showering punch-through background.

4. An indication of how the detector can be used in a beam dump mode at low luminosity. The varying path length through the absorber allows separation and measurement of the pion and prompt muon spectra. Here the specific comparison is between top decay and pion decay. Determination of the background signals leading into the electroweak boson region is essential to understanding that region. Neither CDF nor LAPDOG can operate in the beam dump mode.

5. An estimate of the heavy quark background contribution to Drell-Yan production of dimuons. Also indicated is the need for like-sign dimuon measurement to understand the unlike-sign dimuon signal. LAPDOG cannot distinguish like-sign and unlike-sign pairs.

6. The background from pion decay and punch-through for this proposal and CDF. Both derive from the pion source spectrum of Ref. 1, also shown in the figure. The P-712 background is a factor 15 below the CDF background. Also shown is the muon signal from $W^+$ decay as estimated by CDF[1] and by Paige.[3]

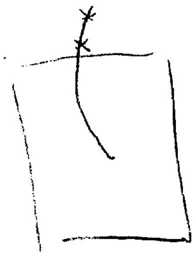

7. The top figure is a schematic of the Coulomb telescope of Ref. 2, pp. 101-104. Fig. 7b gives rejection factors for showering punch-through mimicking a multiply-scattering muon. To estimate our rejection factors we have very conservatively used the square root of F indicated in the figure. See part II, section (e) for discussion.

8. The effect of our momentum resolution ($\sigma/p = \pm 14\%$) on the single muon signal from $W^+$.

9. A comparison of the single muon spectrum seen by this proposal and by CDF. The factor 15 reduction in pion decay and punch-through background gives this experiment a much purer sample of W events.

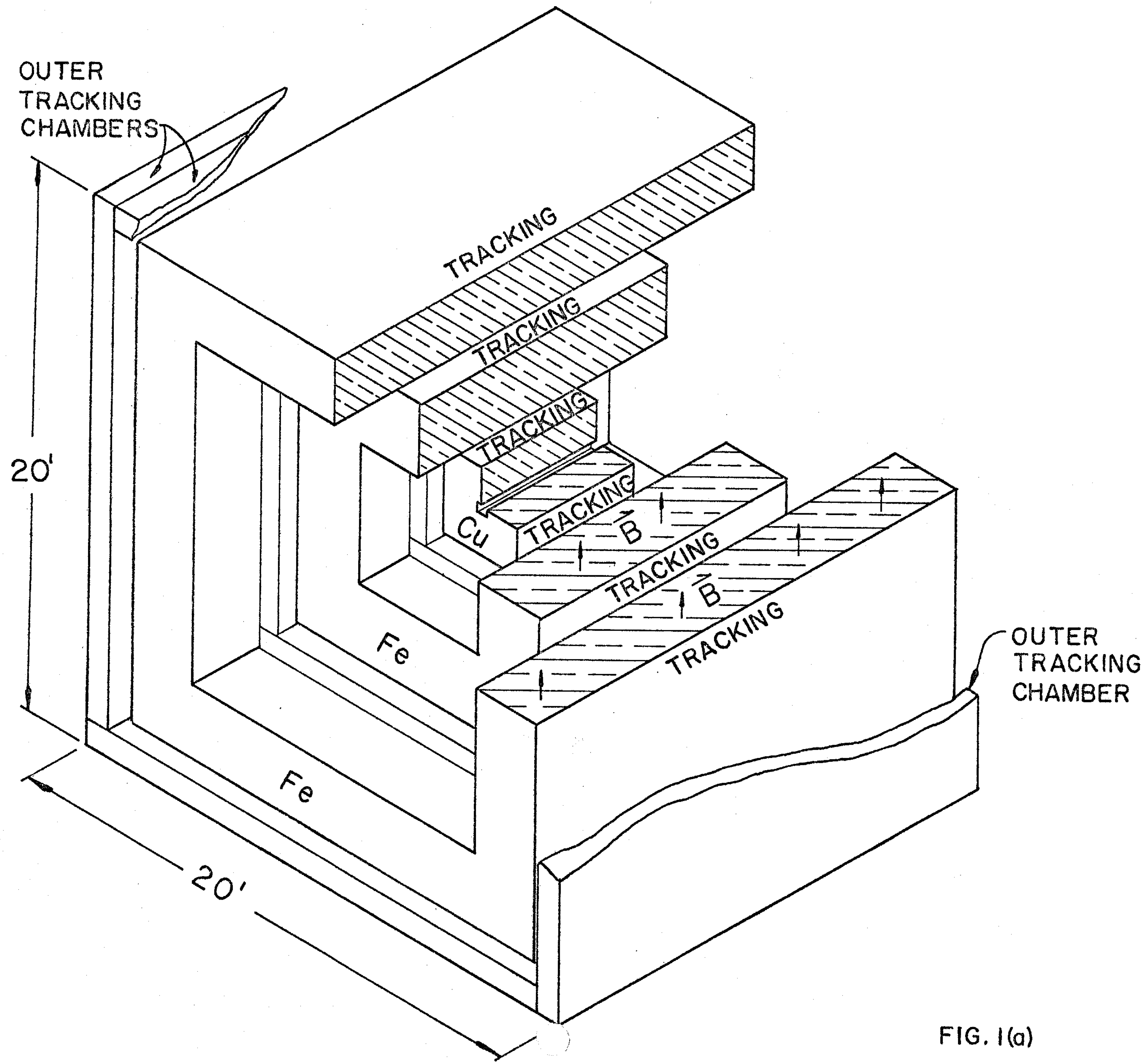
OUTER
TRACKING
CHAMBERS
20'
TRACKING
TRACKING
TRACKING
TRACKING
Cu
TRACKING
$\vec{B}$
TRACKING
$\vec{B}$
TRACKING
Fe
Fe
20'
OUTER
TRACKING
CHAMBER

FIG. 1(a)

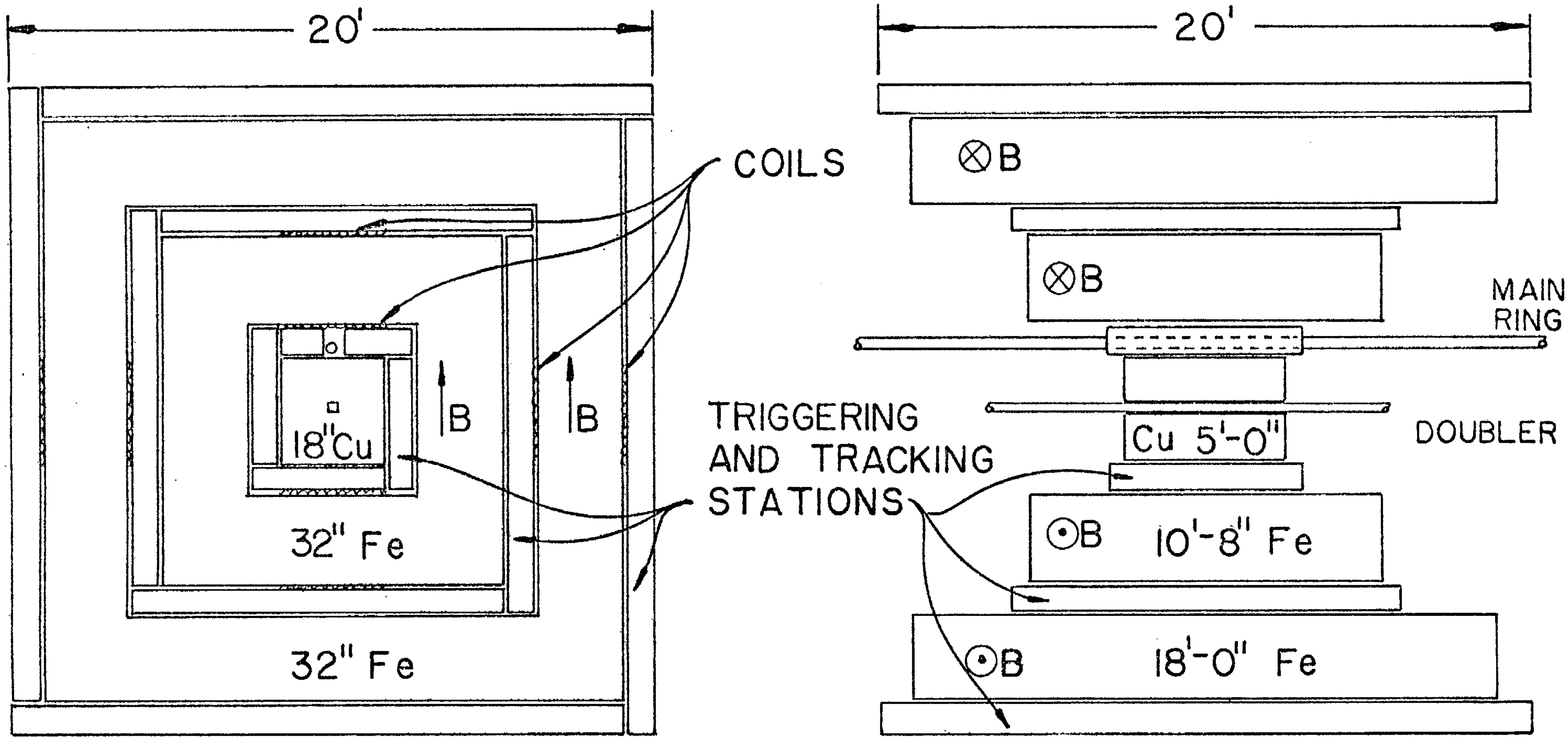


END VIEW

FIG. 1(b)

SIDE VIEW

FIG. 1(c)

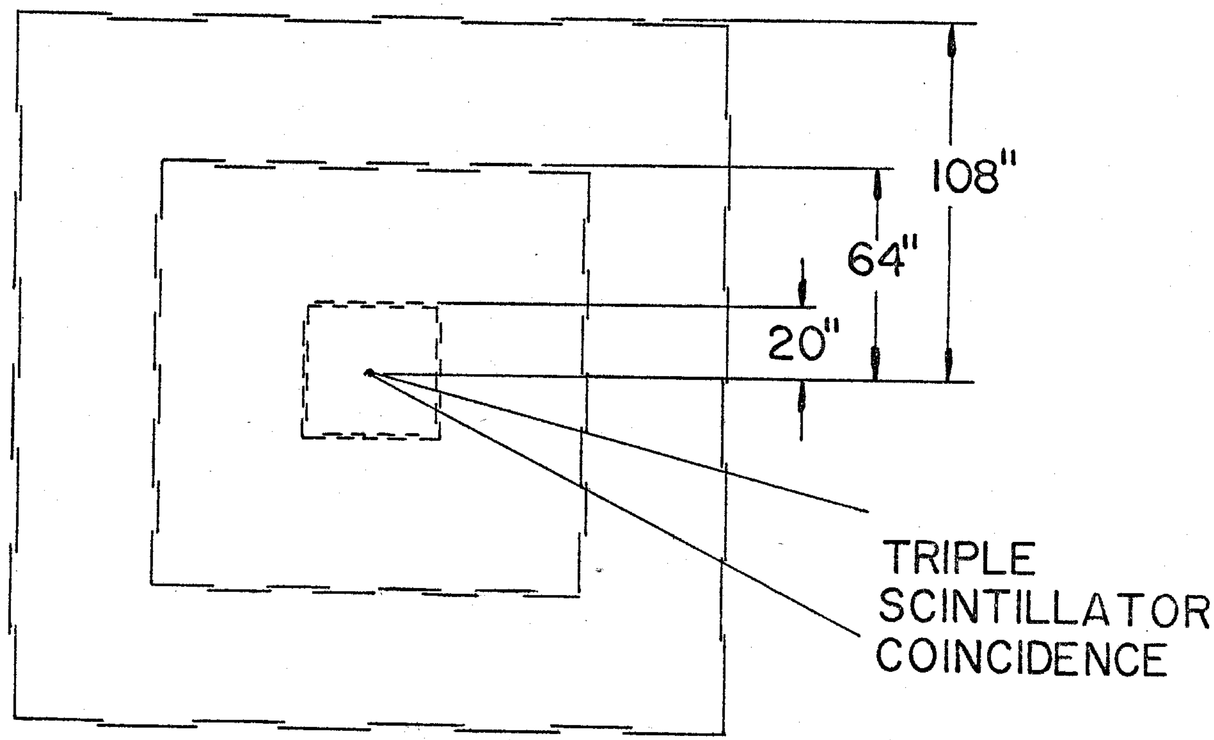


32 TRIGGER TELESCOPES

FIG. 2

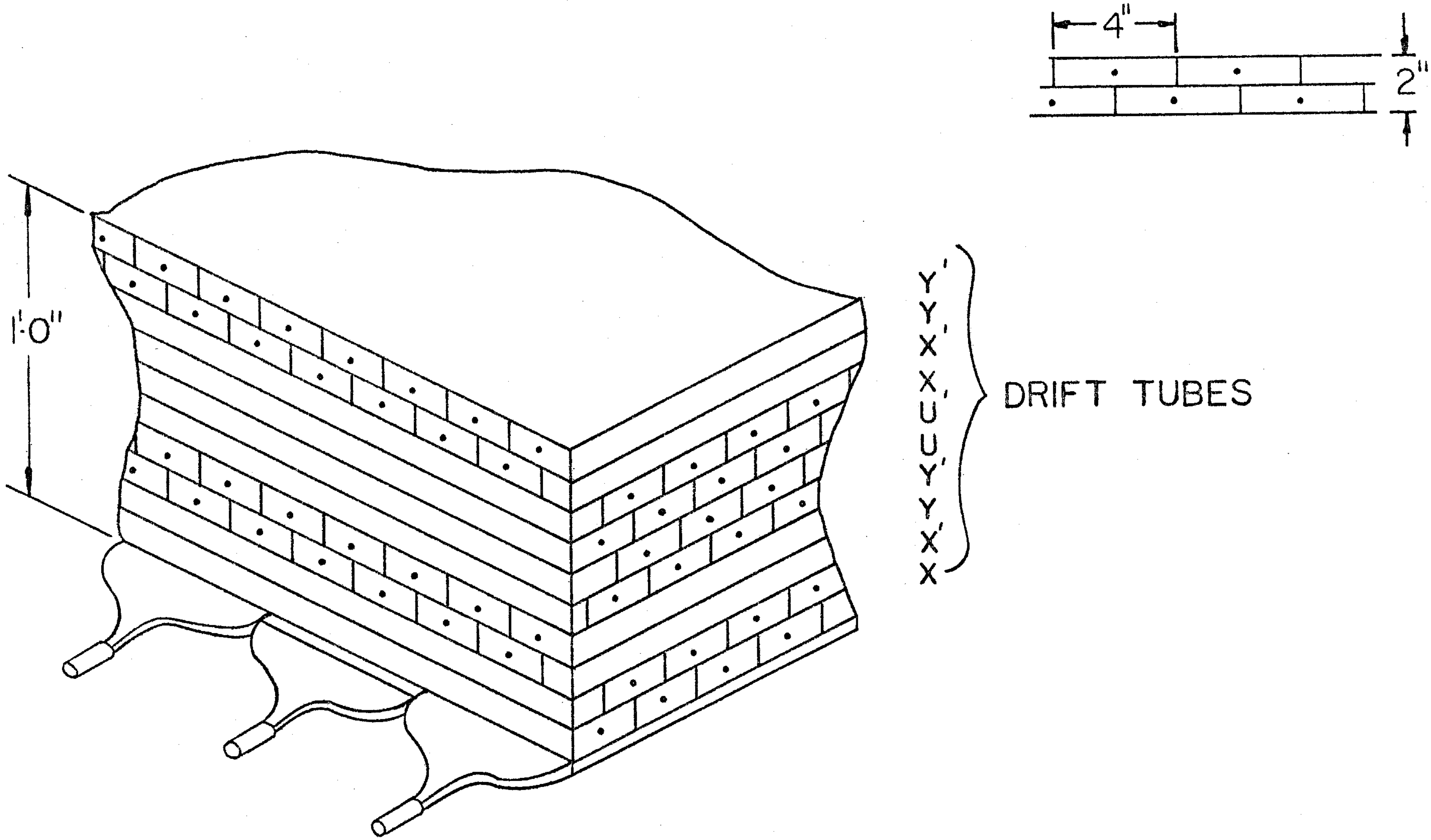


TRIGGERING AND TRACKING STATION

FIG. 3

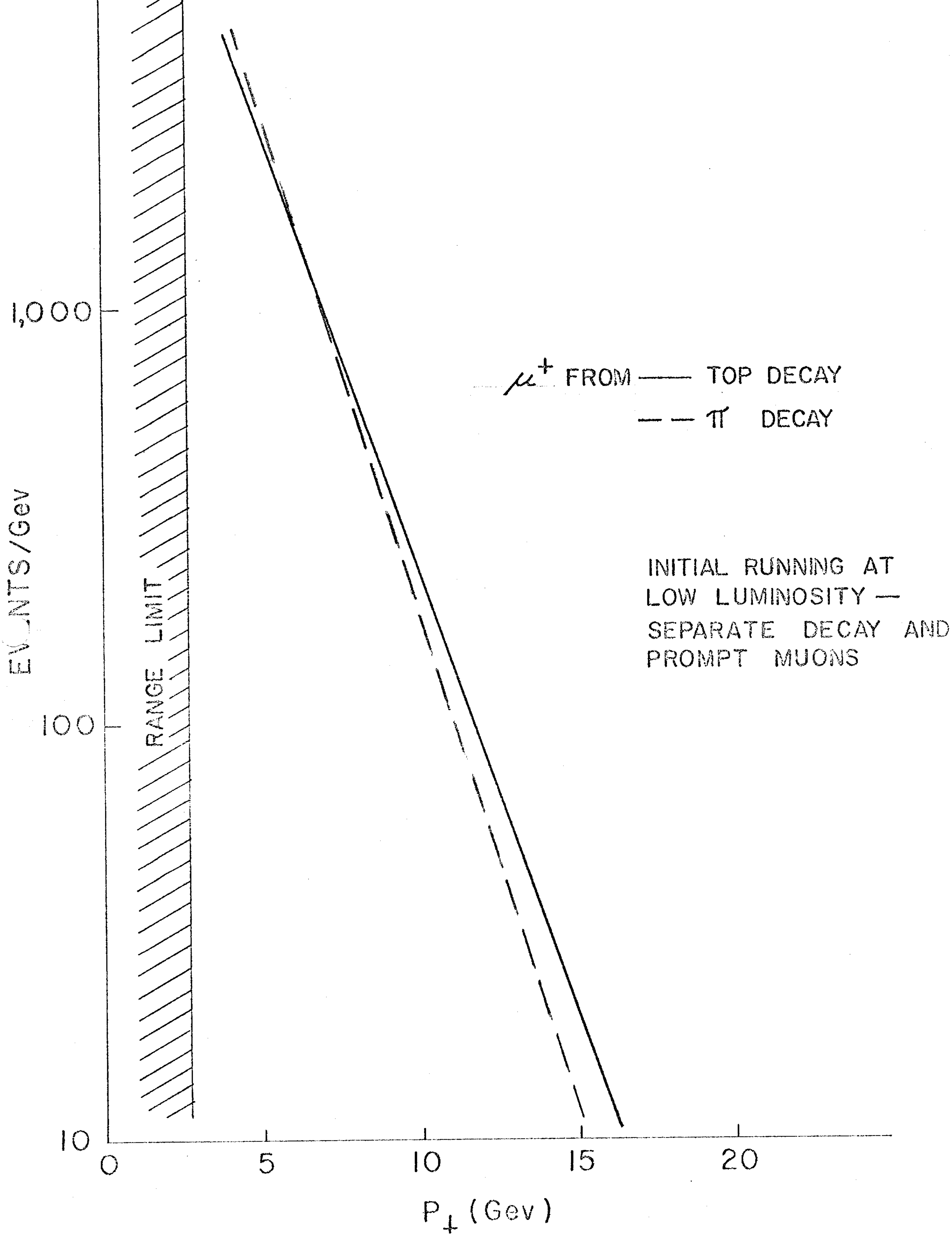

1,000
100
10
0
5
10
15
20
EV_NTS/Gev
RANGE LIMIT
P⊥ (Gev)
μ+ FROM —— TOP DECAY
— — π DECAY
INITIAL RUNNING AT
LOW LUMINOSITY —
SEPARATE DECAY AND
PROMPT MUONS


FIG. 4

DIMUONS

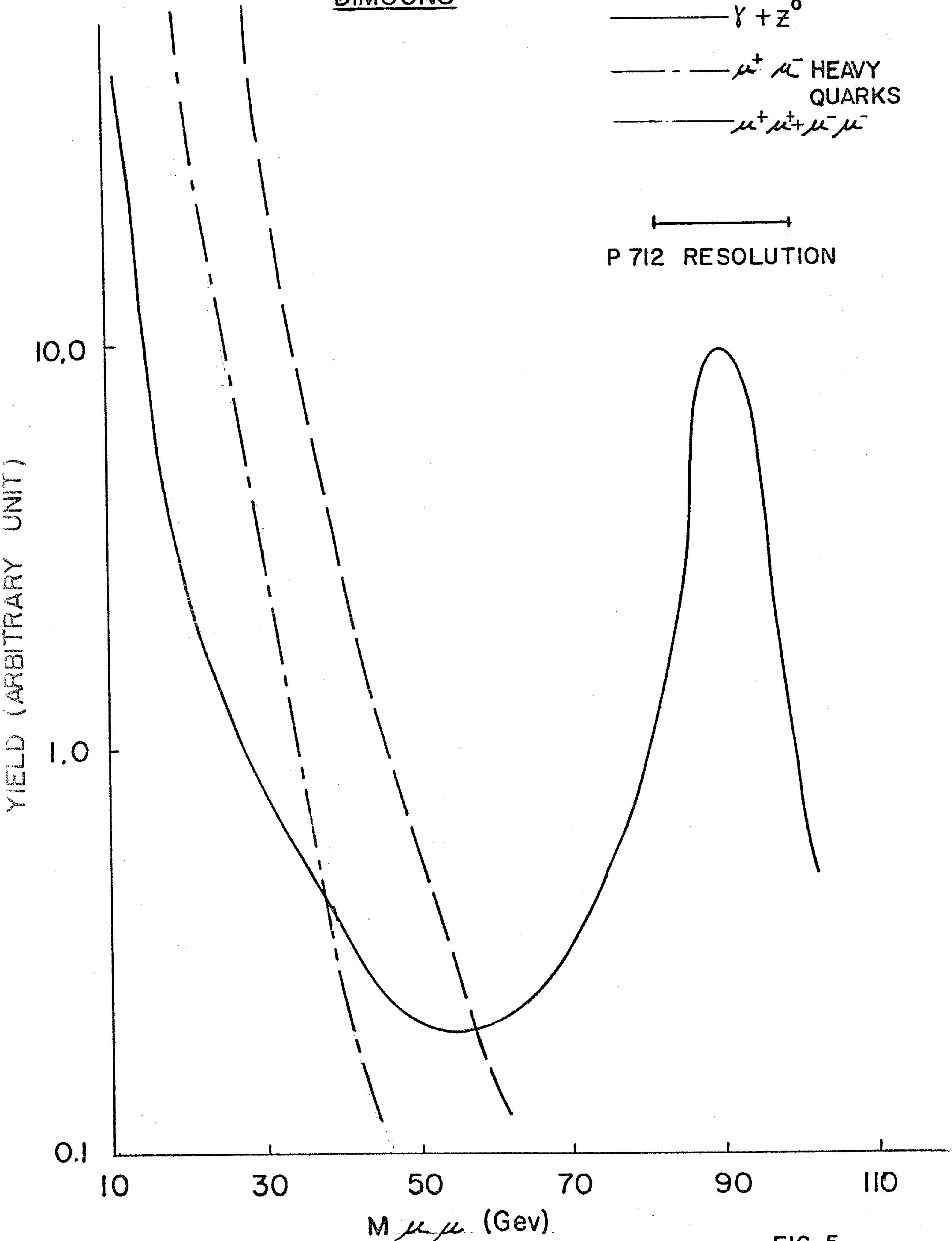


FIG. 5

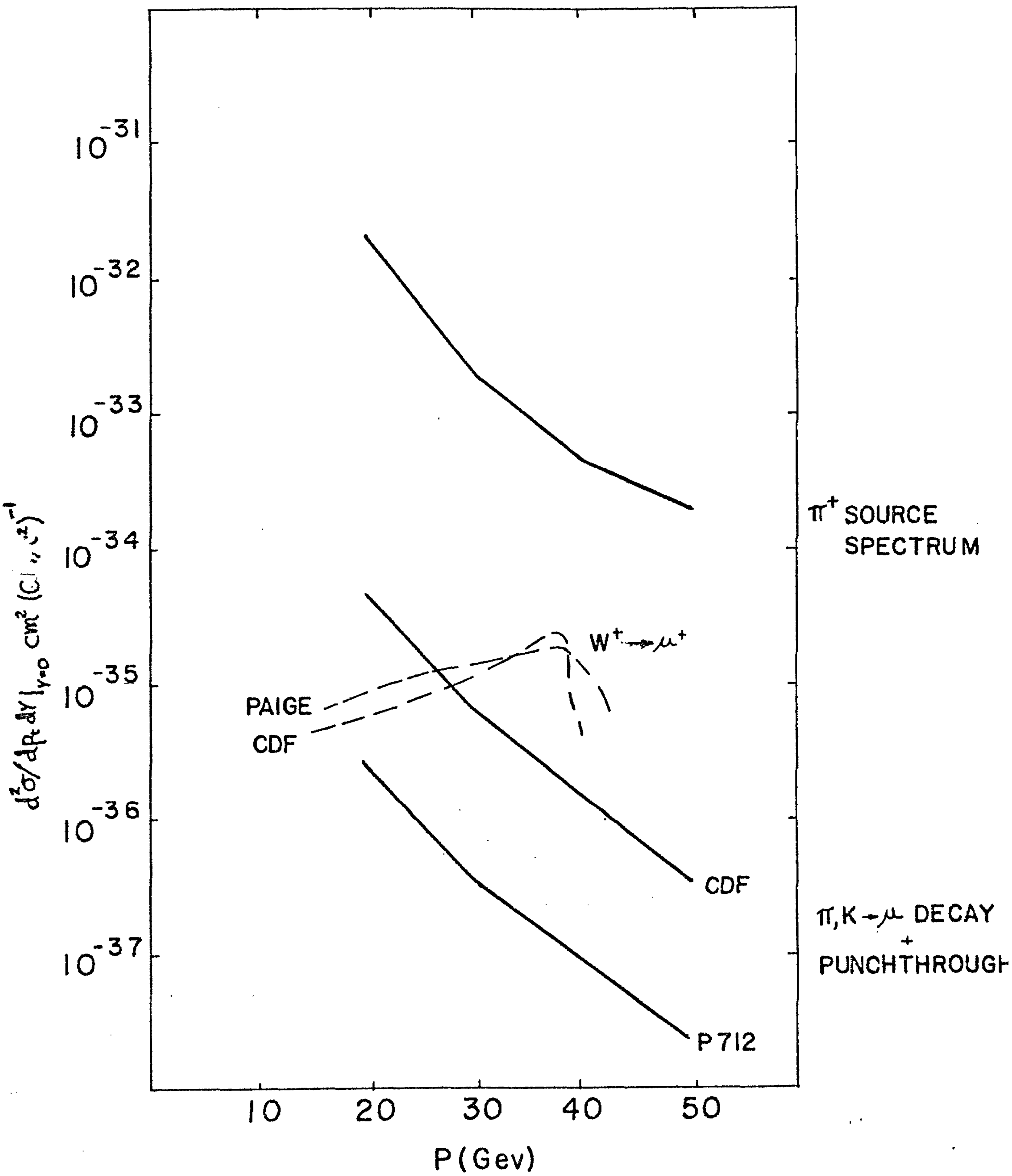

10^-31
10^-32
10^-33
10^-34
10^-35
10^-36
10^-37
10
20
30
40
50
P (Gev)
π+ SOURCE SPECTRUM
W+ → μ+
PAIGE
CDF
CDF
P712
π, K → μ DECAY + PUNCHTHROUGH


FIG 6

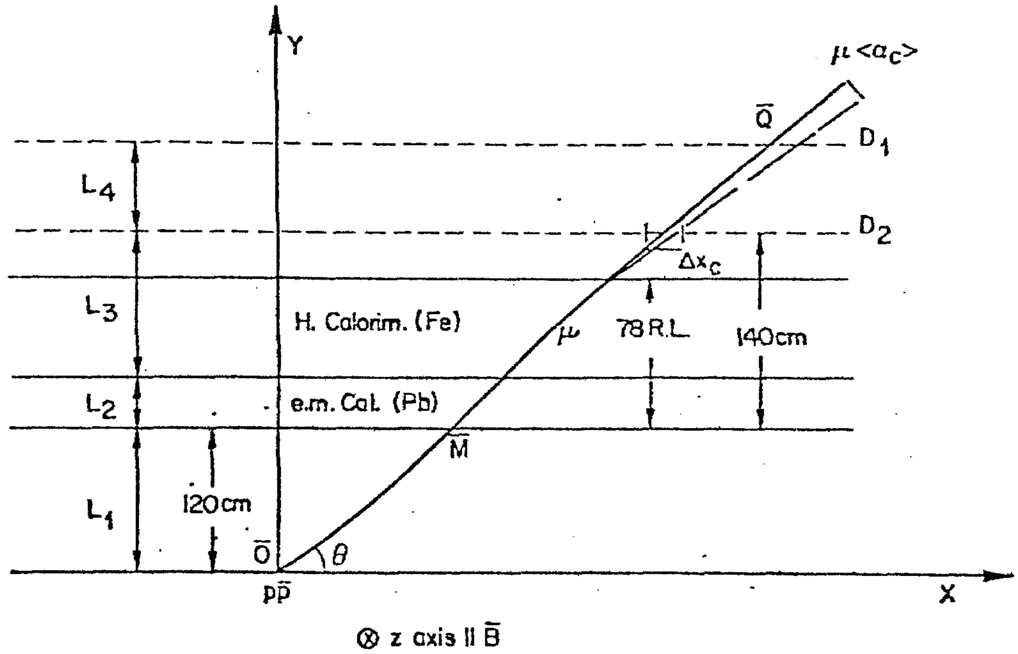


Figure 7 (a) Schematic layout for study of the rejection function F(p). A muon traverses drift chambers $D_1$, $D_2$ with an indetermination $\Delta x_c$ $\Delta y_c$ due to errors reconstructing track $\overline{OM}$ and Coulomb displacement, and Coulomb scattering $<\alpha_c>$. One pion emerging from a hadronic shower in iron has a much larger $<\alpha_H>$ and $\Delta x_H$.

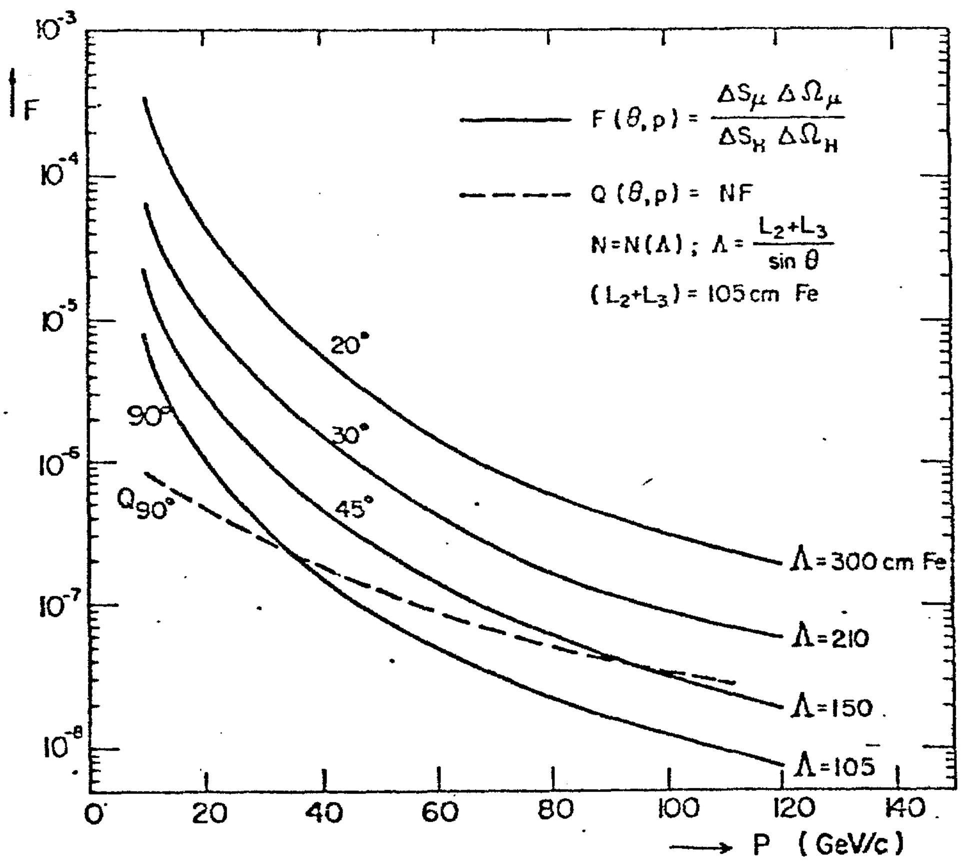


Figure 7 (b) Function $F = (\Delta S_c/\Delta S_H)(\Delta\Omega_c/\Delta\Omega_H)$ probability of having a hadron within the "Coulomb telescope" of a muon. Q = NF(p), total probability as above for N hadrons emerging from the iron in a very high energy event.

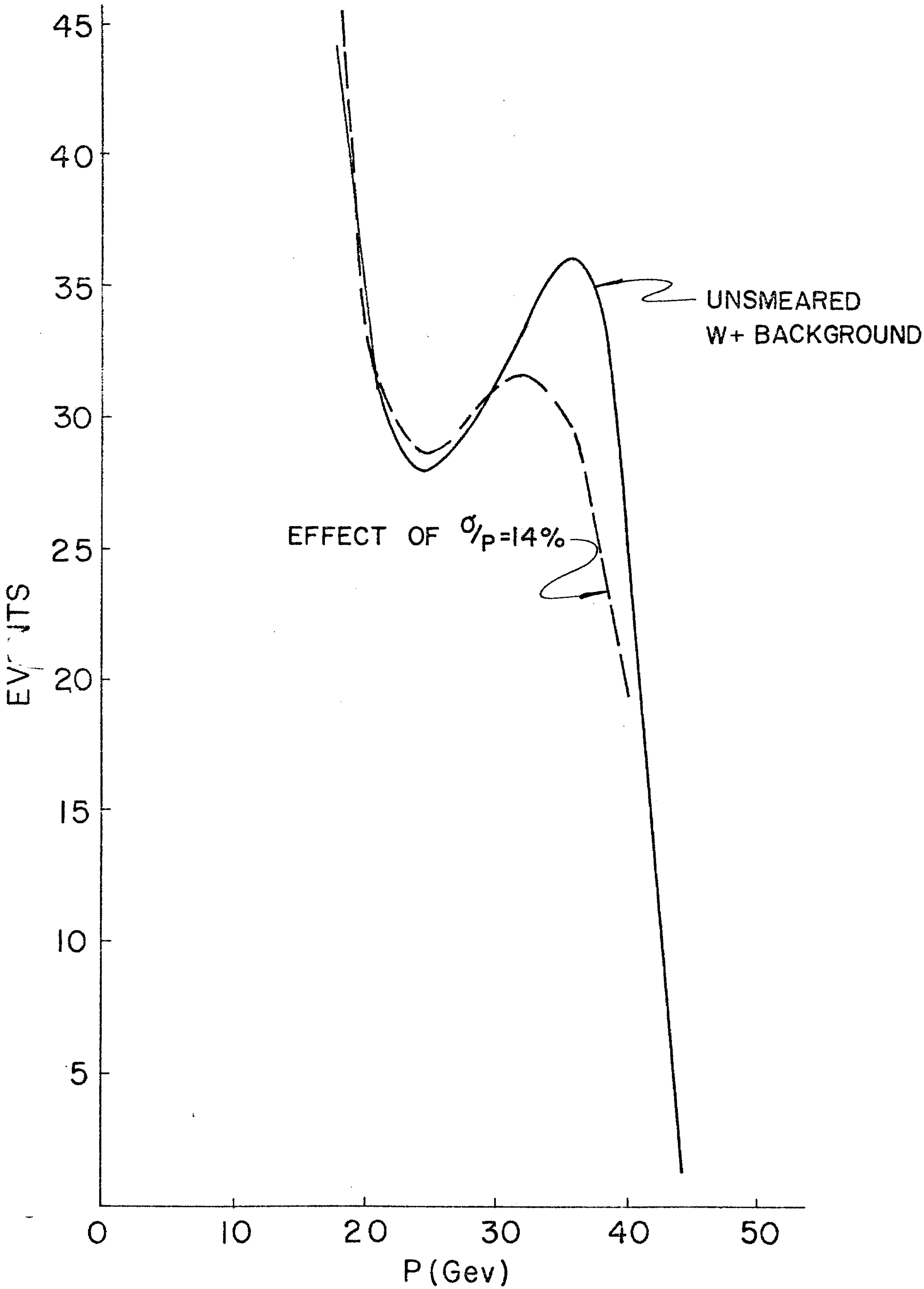


P 712 MOMENTUM SMEARING

FIG 8

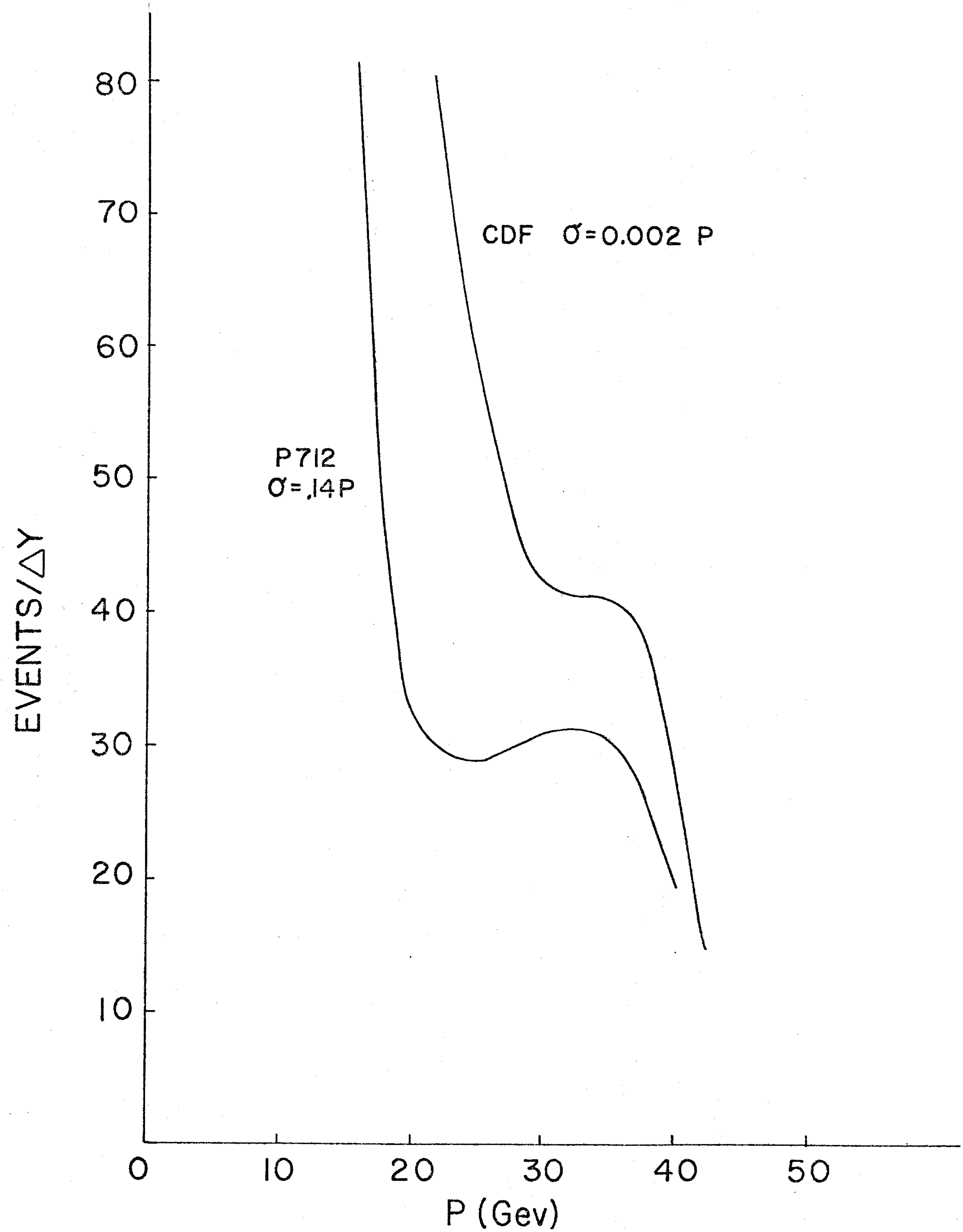


W+ BACKGROUND